Performance and Scaling Analysis of a Hypocycloid Wiseman Engine

by

Priyesh Ray

A Thesis Presented in Partial Fulfillment
of the Requirements for the Degree
Master of Science in Technology

Approved April 2014 by the
Graduate Supervisory Committee:

Sangram Redkar, Chair
Abdel Ra'ouf Mayyas
Robert Meitz

ARIZONA STATE UNIVERSITY

May 2014

ABSTRACT

The slider-crank mechanism is popularly used in internal combustion engines to convert the reciprocating motion of the piston into a rotary motion. This research discusses an alternate mechanism proposed by the Wiseman Technology Inc. which involves replacing the crankshaft with a hypocycloid gear assembly. The unique hypocycloid gear arrangement allows the piston and the connecting rod to move in a straight line, creating a perfect sinusoidal motion.

To analyze the performance advantages of the Wiseman mechanism, engine simulation software was used. The Wiseman engine with the hypocycloid piston motion was modeled in the software and the engine's simulated output results were compared to those with a conventional engine of the same size. The software was also used to analyze the multi-fuel capabilities of the Wiseman engine using a contra piston. The engine's performance was studied while operating on diesel, ethanol and gasoline fuel. Further, a scaling analysis on the future Wiseman engine prototypes was carried out to understand how the performance of the engine is affected by increasing the output power and cylinder displacement.

It was found that the existing Wiseman engine produced about 7% less power at peak speeds compared to the slider-crank engine of the same size. It also produced lower torque and was about 6% less fuel efficient than the slider-crank engine. These results were concurrent with the dynamometer tests performed in the past. The 4 stroke diesel variant of the same Wiseman engine performed better than the 2 stroke gasoline version

as well as the slider-crank engine in all aspects. The Wiseman engine using contra piston showed poor fuel efficiency while operating on E85 fuel. But it produced higher torque and about 1.4% more power than while running on gasoline. While analyzing the effects of the engine size on the Wiseman prototypes, it was found that the engines performed better in terms of power, torque, fuel efficiency and cylinder BMEP as their displacements increased. The 30 horsepower (HP) prototype, while operating on E85, produced the most optimum results in all aspects and the diesel variant of the same engine proved to be the most fuel efficient.

DEDICATION

I dedicate this thesis to my parents and my brother, Javanika and Jitendra Ray, and Radhesh, for their constant support and confidence in me. Their unconditional love has always been an inspiration and a motivation for me to excel in life.

ACKNOWLEDGMENTS

I would like to express my deepest appreciation to my committee chair, Dr. Sangram Redkar, who has the essence of a genius. Without his wise words and persistent guidance, this thesis would not have been possible. His attitude and zest towards teaching has always encouraged me to work harder.

I would also like to thank my committee members, Dr. Abdel Ra'ouf Mayyas and Professor Robert Meitz for being a part of this research.

I would like to thank everyone at the Wiseman Inc. including Keith Voigts, Mark Smith, and Jerry Blankinchip for providing the origin of this thesis: The Wiseman hypocycloid engine.

I am also grateful for the assistance given by Mr. Nigel Fleming at Lotus Simulation Software and John Howell.

Finally, I would like to give a special thanks to all my friends for their tireless effort in encouraging me.

TABLE OF CONTENTS

Page

CHAPTER Page

LIST OF FIGURES

Figure Page

Figure Page

Figure Page

LIST OF TABLES

Table Page

Chapter 1

INTRODUCTION

A unique characteristic of the present day civilization is industrialization, and that has been possible due to the extensive progress in mechanical technology or machines. Most of these machines consume some or the other form of energy and convert them into another. In the simplest form, a machine that does this energy conversion can said to be an engine. This also means that there is a constant need to improve the efficiency of these engines in terms of how they convert the energy from one form to another.

One such engine is the heat engine. A heat engine converts chemical energy stored in a fuel into a thermal energy. This thermal energy is then used to perform work in terms of moving parts. There are primarily two types of heat engines, the external type and internal type. In this study only focuses on the Internal Combustion Engines (ICE). There are various types of ICE invented over the years and their application has varied from generators to locomotives.

Slider-crank Mechanism

Over the course of time, the ICE has undergone incredible change in terms of technical advancements but the fundamental concept behind its mechanism has still remained unchanged. It still relies on the popular slider-crank or crankshaft based mechanism. This mechanism consists of three primary parts. The Crank, which is the rotating flywheel, the piston or the slider that slides inside the tubular cylinder, also known as the bore, and the connecting rod that connects the sliding piston to the crank.

When a mixture of fuel and air enters the cylinder, it pushes the piston down till the entire cylinder is full. This is called the intake stroke. The piston then moves back up to compress the air-fuel mixture, which is known as the compression stroke. Once the piston compresses the mixture the spark plug located at the top of the cylinder ignites the fuel causing it to explode. The energy released from this explosion pushes the piston down again and the whole cycle is repeated. This stroke is also called the exhaust stroke since the exhaust ports are opened during this process to let out the gases formed during the combustion. Mechanically speaking, the linear motion of the piston is converted and transferred to the rotational motion of the flywheel. An IC engine that follows this process can be called a four stroke IC Engine since it undergoes four different strokes, in two revolutions. A visual representation of these four strokes can be seen in Figure 1 below.

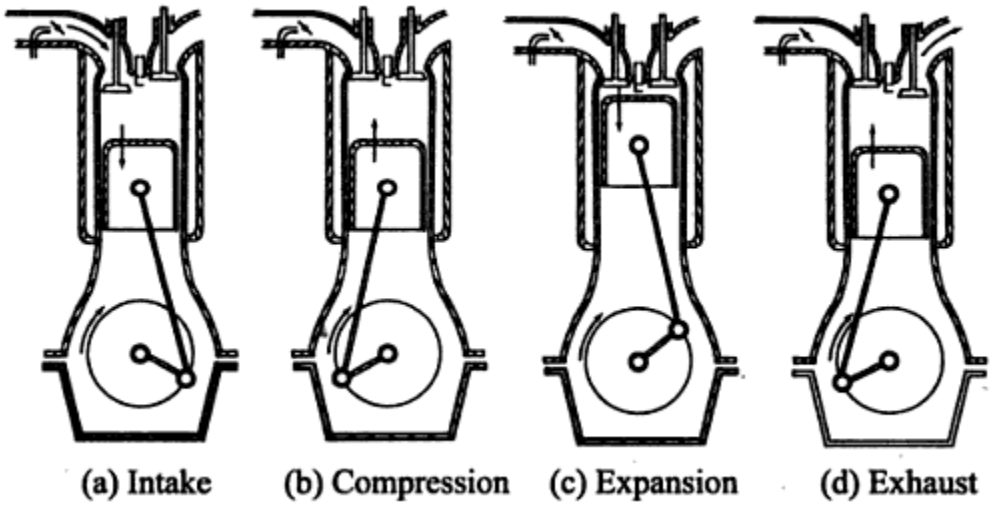

Figure 1 - Working Principle of a Four Stroke SI Engine (Ganesan, 2012, p. 7)

There also exists a two stroke engine in which the entire cycle is completed in one revolution as oppose to the four stroke engines. The main difference between both the

engines is the way the charge is filled and removed from the engine cylinder. In a two stroke engine, the charge entering the combustion chamber is compressed before it is induced into the cylinder which causes the exhaust gases to be pushed out through the exhaust ports. This eliminates the piston strokes required for both these operations.

A diesel engine is slightly different than the spark ignited engine in the sense that, the combustion in the diesel engine is caused due to compression. Hence diesel engines have a much higher compression ratio. The reason behind having a high compression ratio is that the ignition temperature of diesel is lower than gasoline and combustion in the piston chamber can be caused just by supplying energy to the fuel by compressing it. There is no need for an external spark to ignite the fuel in the combustion chamber (Mathur & Sharma, 1997, p. 25).

Despite being the most popular mechanism in the industry, the slider-crank mechanism still has few design limitations. One such shortcoming is the loss of energy due to friction between the piston and cylinder walls. The connecting rod and the piston are joined using a wrist-pin about which the piston is free to rotate. The connecting rod in the slider-crank mechanism follows a sinusoidal motion which is converted into a linear motion at the piston end. As seen in Figure 2, due to the inclination of the connecting rod at various angles, it causes the piston to rub against the inner walls of the cylinder. This produces a load, known as the side load, which is perpendicular to the axis of the cylinder. This load results into reduced engine efficiency due to friction and heat.

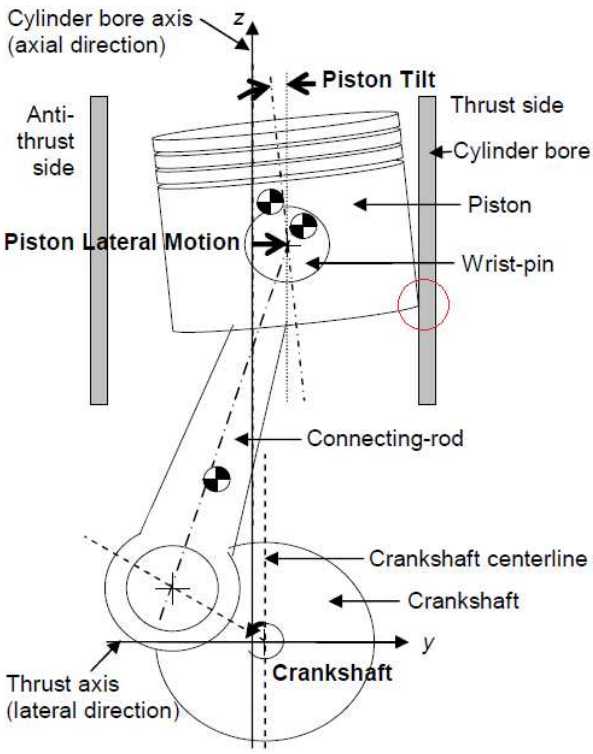

Figure 2 - Piston Side Load

There have been years of research and development to increase engine efficiency and reduce internal cylinder friction. A lot of these solutions to improve the engine efficiency in terms of cylinder friction are often complex and uneconomical. One alternative to this mechanism, especially emphasizing on the reduced cylinder friction, is the Geared Hypocycloid Engine (GHE). The basic theory behind the working of the GHE mechanism is that the crankshaft found in the standard ICE is replaced by a gear assembly. There have been prototypes of the GHE tested in the past and they have proven to be advantageous than the conventional slider-crank setup in terms of efficiency. In order to experimentally further investigate the design benefits of a hypocycloid engine over its slider-crank counterpart, the Wiseman Technologies Inc. (WTI), provided us with

a 30 cc two-cycle GHE. This engine from hereafter will be referred to as the Wiseman engine.

The major tasks required to accomplish this research focus were:

1. Modeling the Wiseman hypocycloid engine.
2. Comparing the Wiseman hypocycloid mechanism to a conventional slider-crank mechanism and understanding the difference between their mechanical assemblies.
3. Analyzing the Wiseman hypocycloid prototype using engine simulation software.
    a. Validating the results generated by simulation software by first comparing it with a stock engine with known performance output.
    b. Simulating the Wiseman engine using the Lotus Engine Simulation (LES) software to determine various performance parameters.
    c. Setting baseline results to which the conventional engine and the Wiseman engine can be compared with.
4. Performing multi-fuel and scalability analysis on the Wiseman engine to predict its performance for future designs.
    a. Determining how the Wiseman engine performs while operating on different fuels.
    b. Determining how various output parameters of an engine change with respect to its size.
    c. Using the scaling methods to predict the theoretical performance of future Wiseman hypocycloid engine designs.

Chapter 2

BACKGROUND

GHE has been a research-interest for many decades now and various universities and groups have contributed to the development of the mechanism. One of the first documented mechanism was produced by an English engineer, James White (Dickinson, 1949-51, p. 175-179). White's engine with its unique gear assembly can be seen in Figure 3. Even though White received a medal from Napoleon Bonaparte in 1801 for his invention, he was not entirely convinced by the design benefits (White, 1822, p. 30-31). But a German mechanical engineer, Franz Reuleaux, is considered to be the originator of the slider-crank as well as the hypocycloid mechanism design. A collection of his various mechanisms which combine different gear systems with a slider-crank is now displayed at the Cornell University. Two of those designs can be seen in Figure 4. Various other steam engines were later produced based on White's and Reuleaux's design. One such engine was developed by Matthew Murray in 1802, which was patented and manufactured to be used as a water pump in 1805 (Karhula, 2008, p. 19). There have been many other famous mathematicians and scientists who have proposed their theories and designs for a modified hypocycloid mechanism or also known as the cardan gear mechanism.

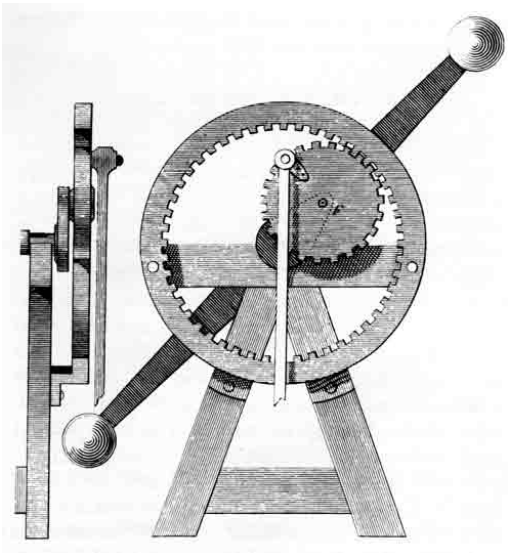

Figure 3 - White's Geared Hypocycloid Engine

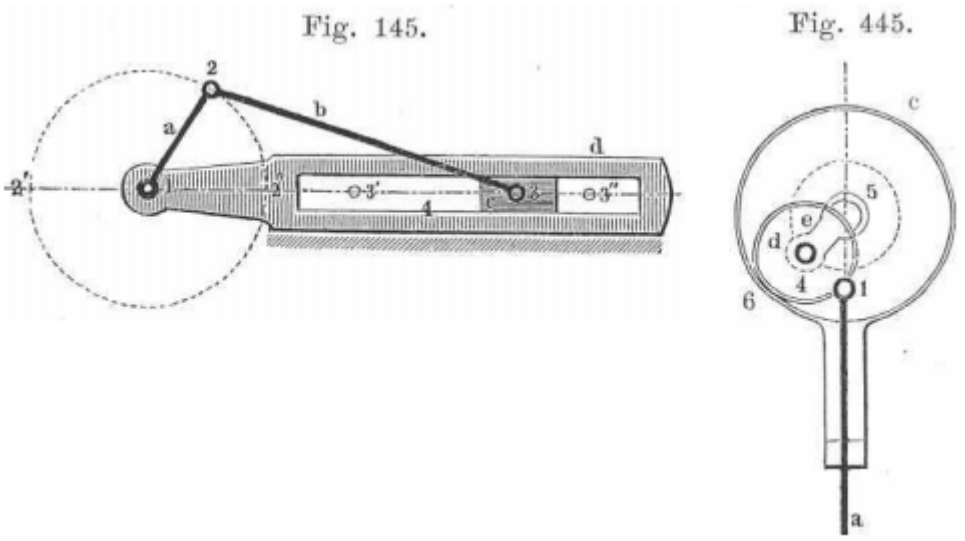

Figure 4 - Franz Reuleaux's Slider-crank (L) and Cardan Gear (R) Mechanisms (Karhula, 2008, p. 20)

Hypocycloid Concept and Geared Hypocycloid Mechanism

To better understand the mechanical movement in a hypocycloid mechanism, it is important to understand the mathematical concept of a hypocycloid curve. A hypocycloid

can be described as a special curve produced by tracing a fixed point 'P' on the circumference of a circle (radius r_a) that is rolled inside a larger circle (radius r_b) (Wolfram MathWorld, 2010).

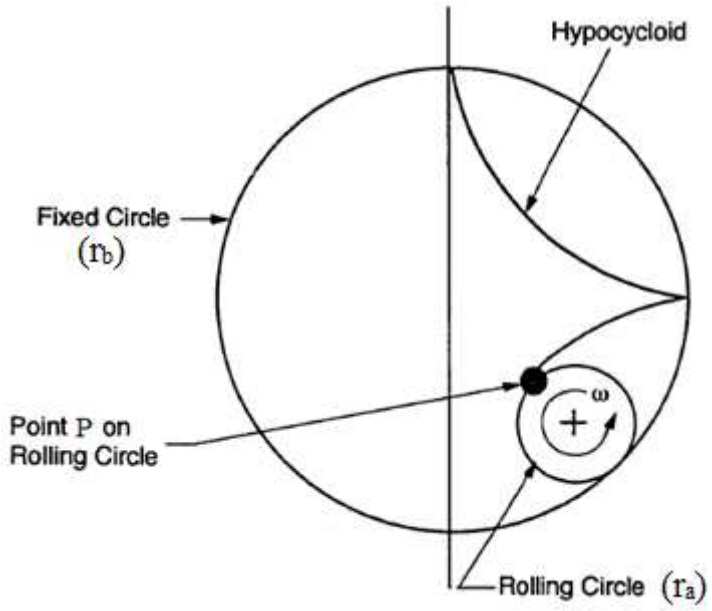

Figure 5 - Hypocycloid Concept

Depending on the ratio of the radii of the two circles, unique hypocycloid curves can be generated. The path of the P can be traced by the following equations;

$$x = (r_a - r_b)\cos\emptyset + r_b \cos\left(\frac{r_a - r_b}{r_b}\emptyset\right) \quad \text{Equation 1}$$

$$y = (r_a - r_b)\sin\emptyset - r_b \sin\left(\frac{r_a - r_b}{r_b}\emptyset\right) \quad \text{Equation 2}$$

Where:

r_a is the radius of the smaller circle.

r_b is the radius of the larger circle.

$\emptyset$ is the angle from the x axis to the line that intersects the center of circle a and circle b.

To benefit from the movement produced by the hypocycloid curve in an ICE, a special case of hypocycloid is utilized. In this case, the diameter of the small circle is exactly half of that of the bigger circle, i.e. 2:1 radii ratio. As seen in Figure 5, when such a ratio of circles are used to trace a hypocycloid curve, as the circle 'a' rolls inside the larger circle 'b' it produces a vertically straight line at any given point on the perimeter of circle 'b'. Further, if the circles are replaced by gears, the assembly can be used in a mechanism to produce a perfect straight-line motion of a piston in an ICE. The device conceived by James White was also based the 2:1 gear ratio in a hypocycloid setting.

Figure 6, gives a better visualization of the straight-line motion produced by hypocycloid gear assembly which has a pitch diameter ratio of 2:1. The smaller pinion gear in red can be compared to the small circle 'a' and the larger internal ring gear represents the larger circle 'b'. As the pinion gear rolls, a specific point located on the pitch diameter always remains coincident with the vertical black line and this is the point which can benefit the piston motion in an ICE.

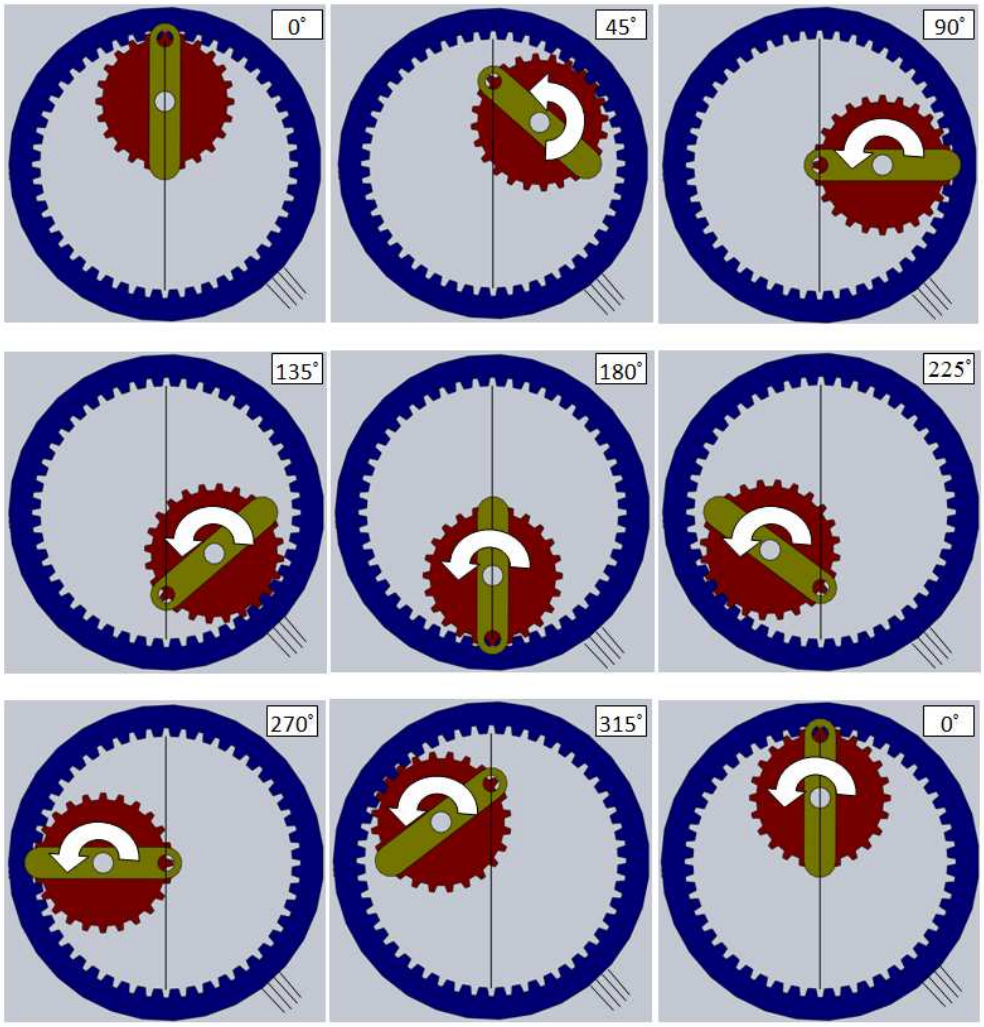

Figure 6 - Geared Hypocycloid Concept Rotating at 45º Increments (Conner, 2011)

Implementing the Geared Hypocycloid Mechanism in an ICE

As discussed above, the 2:1 gear ratio allows any point on the pitch circle of the pinion gear to travel in a perfectly straight line with a perfect sinusoidal motion. But the angle of the straight line depends on the point chosen on the pitch circle. The ICE could benefit from this mechanism after modifying this assembly with addition of few more components. Mr. Randal Wiseman, founder of WTI, filed for a patent in 2001 for an engine incorporating a hypocycloid mechanism. The hypocycloid engine was modified

from a stock 30 cc Homelite engine by adding a link to support the pinion gear where the rotary motion is transferred to an output shaft, known as the rotating output shaft (L2). Further, the bottom end of the connecting rod was connected to the point D1 (Figure 7), and this point represents the previously mentioned point 'P' that traces the vertical straight-line hypocycloidal curve.

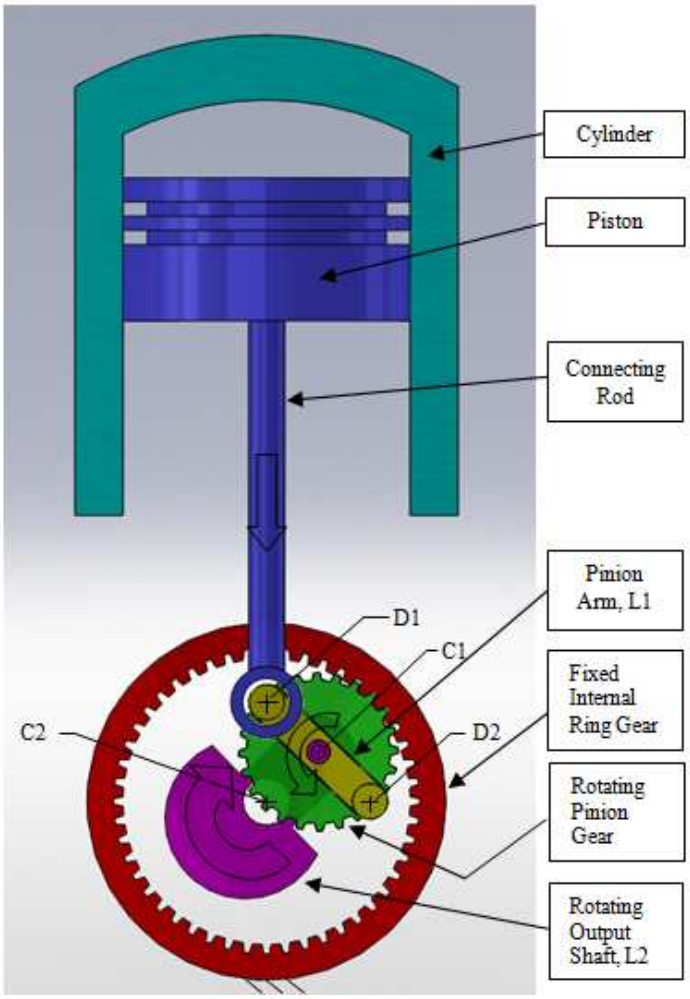

Figure 7 - Schematic of a Single Cylinder G. H. E. (WTI, 2010)

Mr. Wiseman's model proposed in the patent illustrates the link supporting pinion gear (Item 200), known as the carrier shaft (Item 100) in Figure 8 below. The Wiseman

engine also has a provision for the pinion gear teeth (Item 204) to mesh with the fixed internal ring gear (Item 6) in the form of a cavity (Item 322).

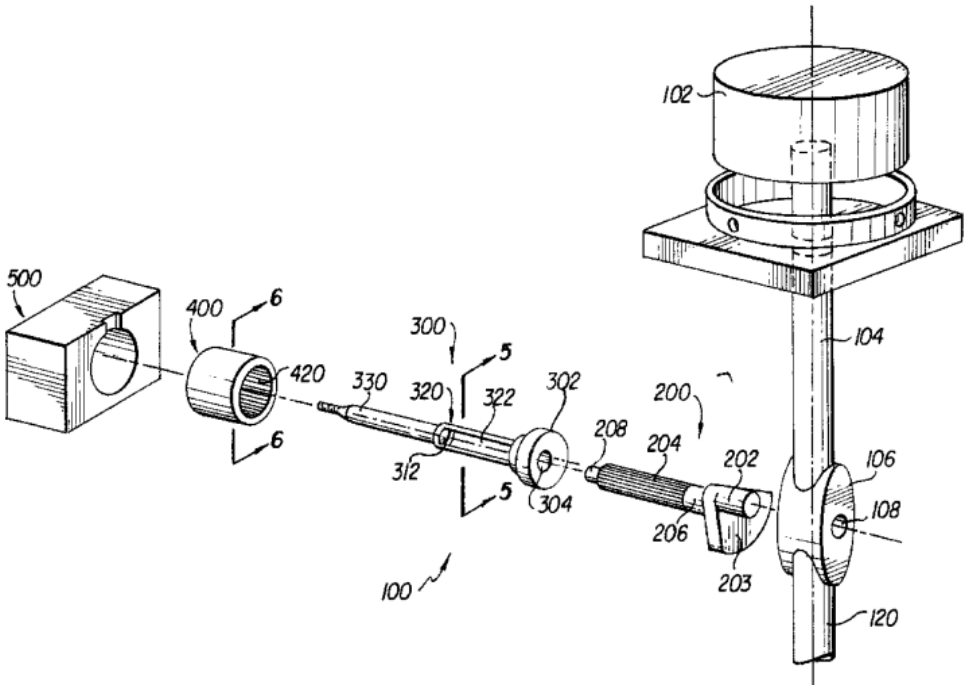

Figure 8 - Sketch from Wiseman US Patent # 6,510,831 (Wiseman, 2001)

Performance Advantages of Hypocycloid Mechanism

Theoretically, the GHE promises various performance and design benefits, with lower friction, heat, and engine vibration being the most important ones. But since there have only been prototypes of such engines and most have not been popularly commercialized, it is important that these theoretical predictions are further explored to gain detailed knowledge of its performance and make more analytical judgments. The cardan gear system is rarely seen in any type of machines (Karhula, 2008, p. 22).

Kenjiro Ishida and Takashi Matsuda studied the basic principles of a geared hypocycloid mechanism which they called a rotation-reciprocation mechanism. In his research attempts, Ishida studied a 63 cc hypocycloid chainsaw engine which he compared it with a conventional slider-crank engine of equivalent size. He declared that the internal gear mechanism was highly practical and tends to produce more power at lesser or equal RPMs as compared to the slider-crank mechanism. After performing various dynamometer tests, he noted that the hypocycloid engine tends to consume more fuel, 751.5 (g/hp)*hr as compared to 295 (g/hp)*hr by the slider-crank mechanism. He reasoned the reduce performance of hypocycloid engine, in terms of brake specific fuel consumption (BSFC), as a result of larger crankcase volume which resulted in lower primary compression ratio (PCR).

While comparing different sinusoidal hypocycloid engines, Ishida also observed that, in terms of design the internal gear assembly in the hypocycloid engines is lucrative when the size is required to be small. Many similar engines even incorporated external gearing to achieve a harmonic motion in a linear path. The flexibility to manipulate the gear size, which determines the overall size of the engine, proves to be beneficial in a case where the dimensions are a design limitation.

Another excellent study of geared hypocycloid engine was conducted by Mr. David M. Ruch as a part of his PhD research. Mr. Ruch, in his PhD dissertation titled “An Experimental and Analytical Investigation of a Single-Cylinder Modified Hypocycloid Engine Design”, mentions that, one of the major benefits of the hypocycloid engine when compared to the sinusoidal engine is that the connecting rod (piston-rod) bending is eliminated. This meant that the force due to gas and inertia exerted on the

piston-rod was only along the rod's axis (Ruch D., 1992). Theoretically, this contributes in increasing the overall of mechanical efficiency of the engine as compared to the conventional engines based on slider-crank mechanism, where the bending forces are produced from the crankpin on the yoke.

One more advantage of the GHE is the reduction in the loads on the crankshaft caused by the gas force (F_g). This is because the torque transmitted in the GHE is split into two paths; one through the crankpin and the other through the sun gear. The total torque then can be expressed as;

$$T' = T'_{crankpin} + T'_{sun} \qquad \text{Equation 3}$$

Where,

T' is total torque exerted on the GHE crankshaft,

$T'_{crankpin}$ is torque exerted on the GHE crankshaft through the crankpin'

T'_{sun} is torque exerted on the GHE through the sun gear.

Further the torque in the crankshaft through crankpin can be expressed as;

$$T'_{crankpin} = F_t' \, (L/4) \qquad \text{Equation 4}$$

Where,

F_t' is tangential load on the modified hypocycloid crankpin from the piston.

Mr. Ruch also mentions that even though all conventional ICEs eliminate most of the piston-skirt/cylinder friction by replacing it with linear bearing friction, there is still approximately 17% energy loss due to the bearing friction. On the other hand, GHE has almost no energy losses due to the linear bearing friction, since the restraining forces caused by the linear bearings in the convention engines are replaced by gear tooth loads

in a GHE (Ruch D., 1993). On the other hand, the gear mesh friction can be reduced significantly since the manufacturing of gears can be highly optimized. Contrastingly the GHE mechanism does result in high gear tooth loads due to the inertia load as a result of pinion rotation about the crankshaft axis (Menz, 1987). For a constant pinion rotational speed, the gear tooth load W_t can be calculated by the following equation;

$$W_t = F_g \, Sin(\theta c) \qquad \text{Equation 5}$$

Where,

W_t is tangential gear tooth load on the pinion,

F_g is gas force on the piston,

θc is crank angle.

Gas force can be calculated by finding the product of the area of the piston head and the pressure exerted on it. In the case of the Wiseman engine, the gas force on the engine piston was known to be 104.4 N. It is also known that this gas force is a function of angle of the crankshaft; therefore it tends to change according to the crank angle. Further, the torque on the output shaft is directly related to the tangential gear load. This relation can be written as;

$$T = (W_t) \, L/2 \qquad \text{Equation 6}$$

Where,

L is Stroke of the engine

T is Torque of the output shaft

Using the above equation, a further comparison between the gas force and relative torque conversion at the output shaft for one full rotation (180º), was also known from the experiments conducted my Mr. Tom Conner and Wiseman Inc. For this purpose it

was assumed that the gas force (F_g) was constant at 1 bar but this is not true in case of a firing engine. It should also be noted that the Wiseman engine stroke is slightly longer at 28.575 mm than the stock engine at stroke at 28.296 mm.

The bore in both the stock and the Wiseman engine measured Ø36.450 mm in diameter and the resulting cross-sectional area is 1043 mm^2. Now by plugging in the described values in the equation 3 and 4, the output torque was calculated an increments of every five degrees of crank rotation. Using this procedure, the stock engine was known to have a higher peak output torque by 1.9% even though it has a shorter stroke. This meant that in a case where the stroke of both the engines were same, that is, 28.575 mm, theoretically the peak output of the stock engine would be about 3% higher than that of the Wiseman engine. Further, from the same experiment, it was known that the peak output torque for the stock engine and the Wiseman engine occurred at 75º TDC and 90º TDC respectively. The stock engine converted gas pressure to torque in a trend that is more typical of a conventional slider-crank engine. The Wiseman engine produced more torque than the stock engine after 85º even though the pressure from the combustion is considerably reduced at this point.

Further the mechanical efficiency of the Wiseman engine was found out to be 0.606 or 60.6%. This was done by examining the results from past dynamometer tests conducted at MTD Southwest, Inc. During those tests, it was found that at 7000 RPM the Wiseman engine had a loss of 0.39 HP due to friction. Whereas the engine was designed to generate 0.99 HP as peak power at 7000 RPM. All this information is crucial in modeling the Wiseman engine using the LES software as it provides more realistic results hence making it more accurate.

Chapter 3

SCOPE OF WORK

Prior to this research, extensive designing, development, testing and modifications of the Wiseman engine were completed by the Wiseman Technologies Inc. and Mr. Thomas Conner. The purpose of this research effort is to further evaluate and tune the Wiseman engine according to the current industry standards to determine any necessary modifications required to enhance the performance. The Wiseman engine was designed on a platform of a 30 cc Homelite brand string trimmer engine. The data for the unmodified (stock) 30 cc Homelite engine was also made available by WTI to be used as an established benchmark. This data will be used to evaluate the performance against the Wiseman engine. The particular Wiseman engine that is discussed in this paper was previously studied for vibration testing and balancing, so these aspects of the engine performance will not be focused on. Hence, it was assumed that the engine is perfectly balanced prior to starting this research.

Modeling the 30 cc Wiseman Hypocycloid Engine

All the required engine parts to assemble a balanced Wiseman prototype were made available by WTI to perform further testing. Since the Homelite engine acted as the platform to build the Wiseman prototype, the prototype retains many of the original Homelite engine's components and dimensions. This similarity is further evident in the side-by-side photo of both the engines seen in Figure 9.

Figure 9 - Wiseman (Left) and Stock Engine (Right)

Both the engines share the same carburetor, ignition system, flywheel/magneto, exhaust/muffler, and the cylinder. The following table provides a summary of their design specifications.

Engine	Stroke	Bore Ø	Displacement
Wiseman Prototype	1.125 in (28.6 mm)	1.435 in (36.5 mm)	1.819 in^3 (29.81 cc)
Stock Homelite	1.114 in (28.3 mm)	1.435 in (36.5 mm)	1.802 in^3 (29.53 cc)

Table 1 - Engine Specifications

The section view of the dynamic CAD model of the Wiseman engine, as seen in Figure 10, shows the mechanical assembly of Wiseman engine for better visualization.

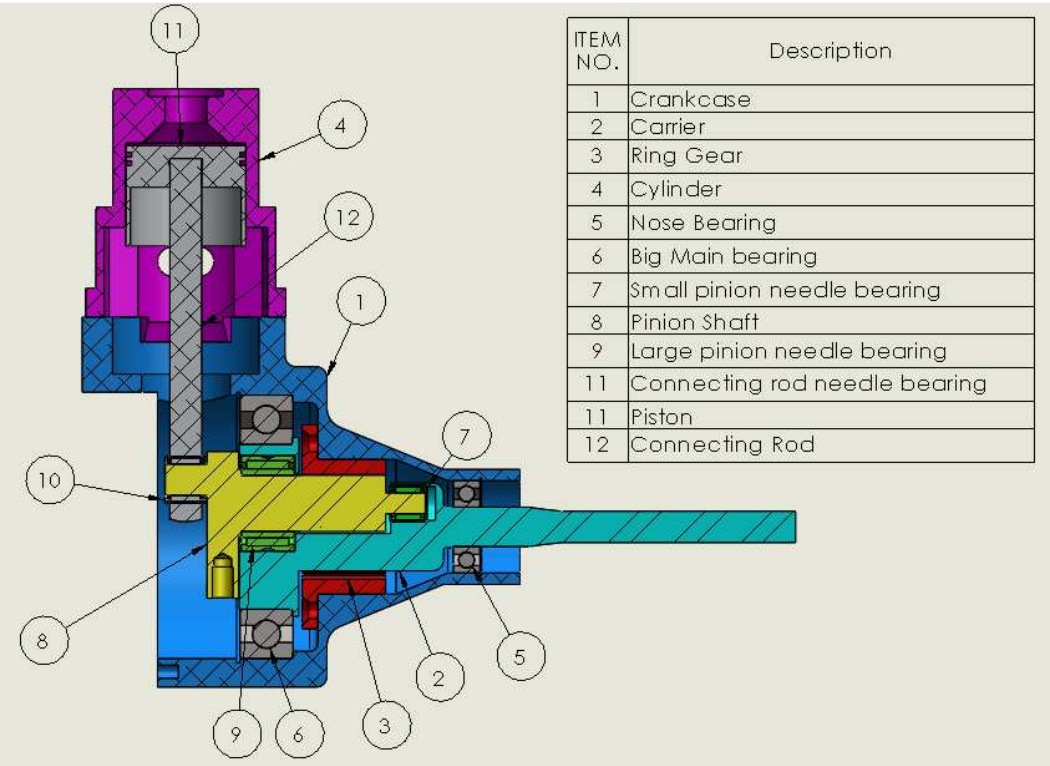

ITEM NO.	Description
1	Crankcase
2	Carrier
3	Ring Gear
4	Cylinder
5	Nose Bearing
6	Big Main bearing
7	Small pinion needle bearing
8	Pinion Shaft
9	Large pinion needle bearing
11	Connecting rod needle bearing
11	Piston
12	Connecting Rod

Figure 10 - Wiseman 30 cc Prototype Section View (Conner, 2011)

Note that the front shaft seal, engine back plate, spark plug, rings, and cylinder cooling fins are not shown in the Figure 10. The crankcase (Item 1) is machined from 6061-T6 billet Aluminum and provides the main support for the engine. The primary supporting bearings of the carrier shaft are the nose bearing (Item 5) and the big main bearing (Item 6). These bearings are held in place by cir-clips in the crankshaft (not shown). The connecting rod bearing (Item 10) is held in place by mild press and is also glued to the base of the connecting rod. The piston (Item 11) and the connecting rod (Item 12) are also machined from 6061-T6 billet Aluminum. Both these items are screwed together using undercut threads for frictional fit. The primary output shaft of the engine, carrier shaft, is machined from 1045 Steel and so is the pinion shaft (Item 8). The

pinion shaft plays multiple roles; it comprises of the external gear teeth, provides bearing surface for the connecting rod and carrier shaft, and also acts as a counterweight. These gear teeth mesh with the internal teeth of the ring gear (Item 3). This geared driveline can be seen in Figure 11. The pitch diameter of the pinion shaft gear is 14.2875 mm (0.5625 in) and that of the ring gear is 28.575 mm (1.125 in). This gives a perfect 2:1 ratio required for the hypocycloid motion.

The Following Figures provide different views of the Wiseman engine for one full rotation at 90º increments, to depict the working of this mechanical assembly.

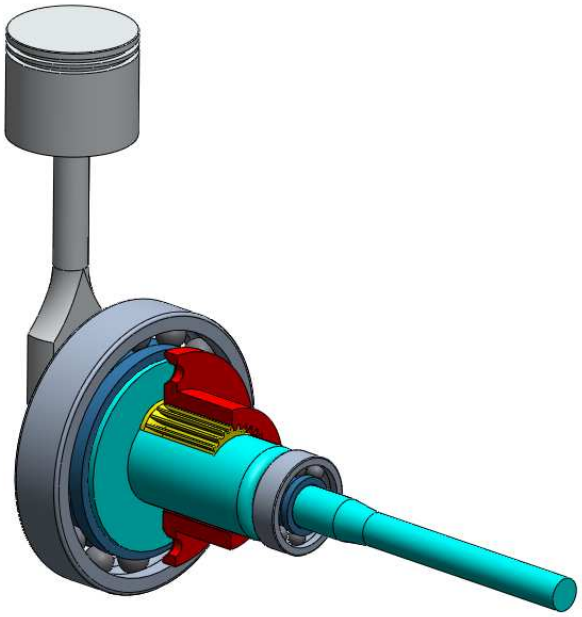

Figure 11 - Wiseman Driveline (Conner, 2011)

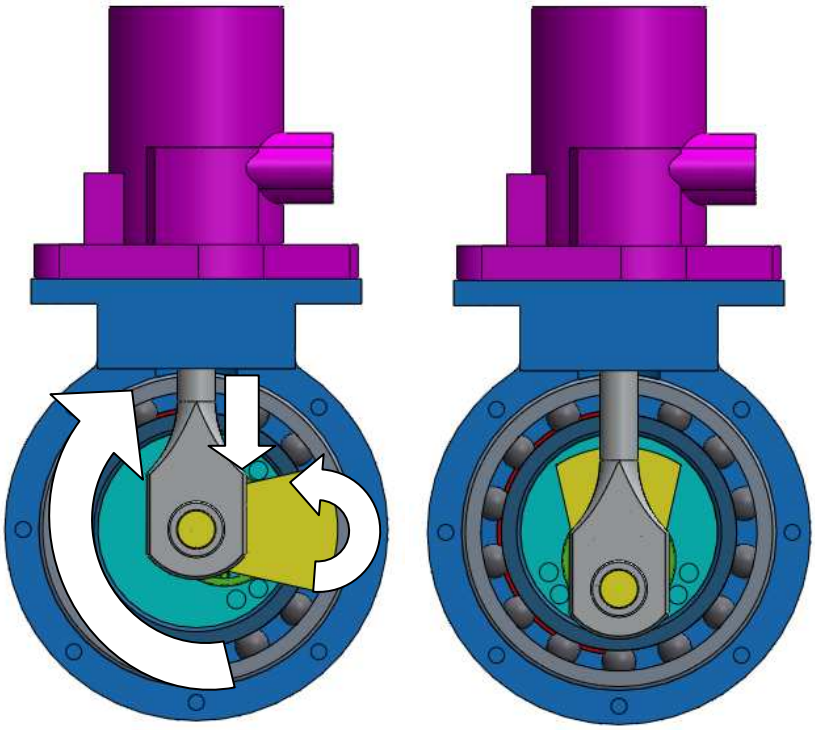

Figure 12 - (Left) Back View, Engine at 90º ATDC (Conner, 2011)

Figure 13 - (Right) Back View, Engine at BDC (Conner, 2011)

Once again, it can be noticed from Figures 12 and 13 that the connecting rod remains vertical and the pinion shaft is both rotating and at the same time oscillating vertically. Another observation that can be made is that the pinion shaft and the carrier shaft rotate in the opposite direction but at the same speed. This means that the pinion shaft bearings manage the loads at twice the speeds of the output shaft, and so is a very crucial component of the engine.

Prior Tests by Wiseman Technologies Inc.

WTI mainly focused on the fuel efficiency as a measure of engine performance on both, the stock engine and the Wiseman prototype. These tests were conducted on low

speeds of about 4000 RPM and at less than wide open throttle. The peak power speeds of such engines are about 7000 RPM. WTI's tests showed that the Wiseman engine could achieve twice the fuel efficiency of the stock engine. Both the engines tested by WTI were brand new so they had to be broken in. In order to do so, they ran both the engines at 4000 RPM with 30:1 gas to oil ratio (2-cycle oil) for about 2 hours. They then changed the fuel and oil to Shell High Test, and AMS synthetic oil with a new ratio of 100:1. For a more systematic test procedure, they took the climate into consideration, and so both the engines were tested on the same day under similar temperature and barometric weather conditions. The test speed for the engines was set to 4050 RPM, and 20" X 6 wooden propeller was used as a load for both the engines. Once they attained stable speeds the cylinder temperature (using thermocouples) and fuel consumption was measured. A series of 6 minute long tests were conducted and the following results were produced (Wiseman Technology, Inc.):

Engine	Temperature (cylinder head)	Fuel Consumption	Run-time
Stock Engine	310˚F	27.67 grams	6 minutes
Wiseman Engine	320˚F	14.00 grams	6 minutes

Table 2 - Summary of Engine Tests Conducted by WTI

They noted that the Wiseman engine, while producing the same output power, ran for virtually twice as long as the stock engine for the same amount of fuel. Based on this time test, along with the fuel consumption measurements, WTI claimed that the Wiseman engine was 50.5% more fuel efficient than the unmodified stock engine. They also noted that the Wiseman engine ran much cooler than the stock engine.

Chapter 4

LOTUS ENGINE SIMULATION

Validating LES Results

LES software has the capability to investigate the performance of an internal combustion engine and give predictions of engine output under various conditions. These results can be fuel efficiency, power output, torque, and running temperature of the engine over a period of time. LES allows the entire system to be built and simulated, complete from engine intake to exhaust. This proves to be an economical and convenient method to research and develop internal combustion engines. Since the LES software has been extensively used for this research to predict the performance of the Wiseman engine, it was important that the authenticity of the results generated by the software was confirmed before drawing any conclusions. For the same purpose, a test engine with known parameters and output was tested. The results from that test were then compared to the results generated by modeling that engine in LES software. A small stand alone test engine, manufactured by GUNT Hamburg was provided by the Arizona State University (ASU) for that test procedure. The engine came connected to a test stand for single cylinder engines which was also manufactured by GUNT Hamburg. The test stand was equipped with an eddy current dynamometer which was connected to a computer that recorded various output parameters of the engine during a running test. The results from dynamometer test along with the engine specifications provided by the company were then compared with the LES results. This test engine setup will be referred to as “GUNT engine” from here on. Figure 14 shows the schematic of the methodology for the coming

tests. A speed vs. output torque tests were conducted on the GUNT engine and the results were recorded. The test results were then compared to the engine output specification provided by the manufacturer, which in turn were compared with the simulated results of the engine system modeled in LES. This is to check how close the engine performance results, generated by LES, are to the actual engine performance and those claimed by the manufacturer. Once the relationship between the LES results and test results was confirmed, the LES software was then used to analyze the performance of the Wiseman engine and also to predict the performance of future Wiseman engine designs.

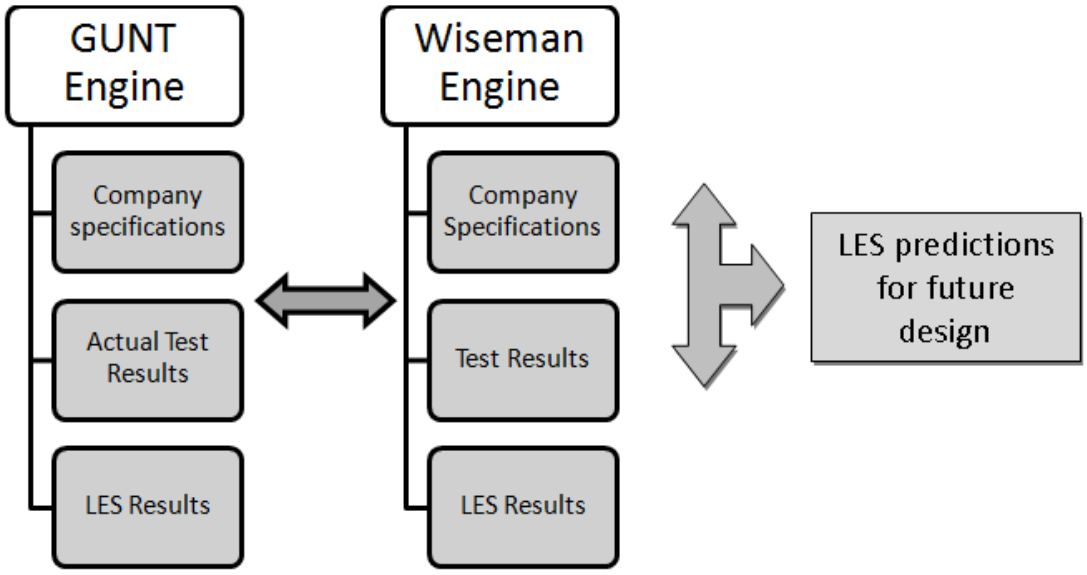

Figure 14 - Methodology to Validate LES Results

GUNT Engine Dynamometer Testing

Figure 15 - GUNT 1B30 Engine

The GUNT engine model 1B30 as seen in Figure 15 was used in conjunction with the CT 110 test stand (not shown). It is a four stroke, single cylinder, air-cooled engine, with direct injection that works on both, diesel and biodiesel fuel. The compression ratio for this engine is 21.5 with a mean piston speed of 6.9 m/s. This is slightly higher than the ideal compression ratio for small four-stroke compression-ignition engines. The compression ratio of such engines generally ranges from 16-20. On the contrary, the bore size of the GUNT engine is smaller than that of a similar sized engine, which is generally 75 to 100 mm (Ganesan, 2012). However, the GUNT engine has a bore diameter of 80 mm.

Some other technical specifications of the GUNT engine are;

Power	Stroke	Bore Ø	Displacement
5.5 Kw @3500 RPM	69 mm	80 mm	347 cc

Table 3 - GUNT Engine Specifications

According the manufacturer the idling speed of this engine is around 800-1000 RPM and the peak power is generated between 3000-3500 RPM. Figure 16 shows the performance curves of the GUNT engine, in terms of power output, torque, and brake specific fuel consumption (BSFC), as claimed by the manufacturer.

Figure 16 - Manufacturer Provided Performance Curves of GUNT Engine

The GUNT engine is mounted on a base plate on the test stand and is coupled with an electric motor via an elastic claw coupling. The electric motor provides force transmission to brake via the elastic claw coupling and is also used to load the engine during the dynamometer testing. The air cooling is provided by the means of blades that are attached to the flywheel of the engine. In addition to all this, the engine comes fitted with various sensors to measure, ignition cut-off, fuel supply, exhaust gas temperature and speed.

Once various components and features of the GUNT engine were understood, setting up the test equipment was fairly simple. Contrary to the claims by the manufactures, the engine needed to be cranked at 2500 RPM and at wide open throttle. A dynamometer test was conducted to get a torque vs. RPM curve. In order to do this, the engine was kept at a constant throttle (WOT) and along with constant torque. The engine was then loaded with different RPMs to see how the change was reflected in the torque output. These points were then recorded to get a curve on a plot. The data collected from these tests was then compared with that provided by the manufacturer. It was found to be very similar to the specification sheet. The range of RPM that the engine was tested at was 1500 to 3500. The engine was then modeled in the LES software to compare the results from the software with that from the dynamometer test and manufacturer data.

GUNT LES Modeling

Once the GUNT engine was tested on the dynamometer, it was then modeled in the LES software with all manufacturer specified parameters. Some crucial engine details were not provided by the manufacturer like, the length of the connecting rod and the intake and exhaust port diameters and their respective valve timings. These parameters significantly affect the performance of the engine in terms of output torque and power.

In order to model the GUNT engine with the most accurate length of the connecting rod, port diameters and valve timings, the lotus ‘concept tool’ was used. As seen in Figure 17, the ‘concept tool’ requires the user to enter at least the following three specifications:

- Engine RPM at maximum power

- Engine Swept volume (liters)
- And the number (no.) of cylinders.

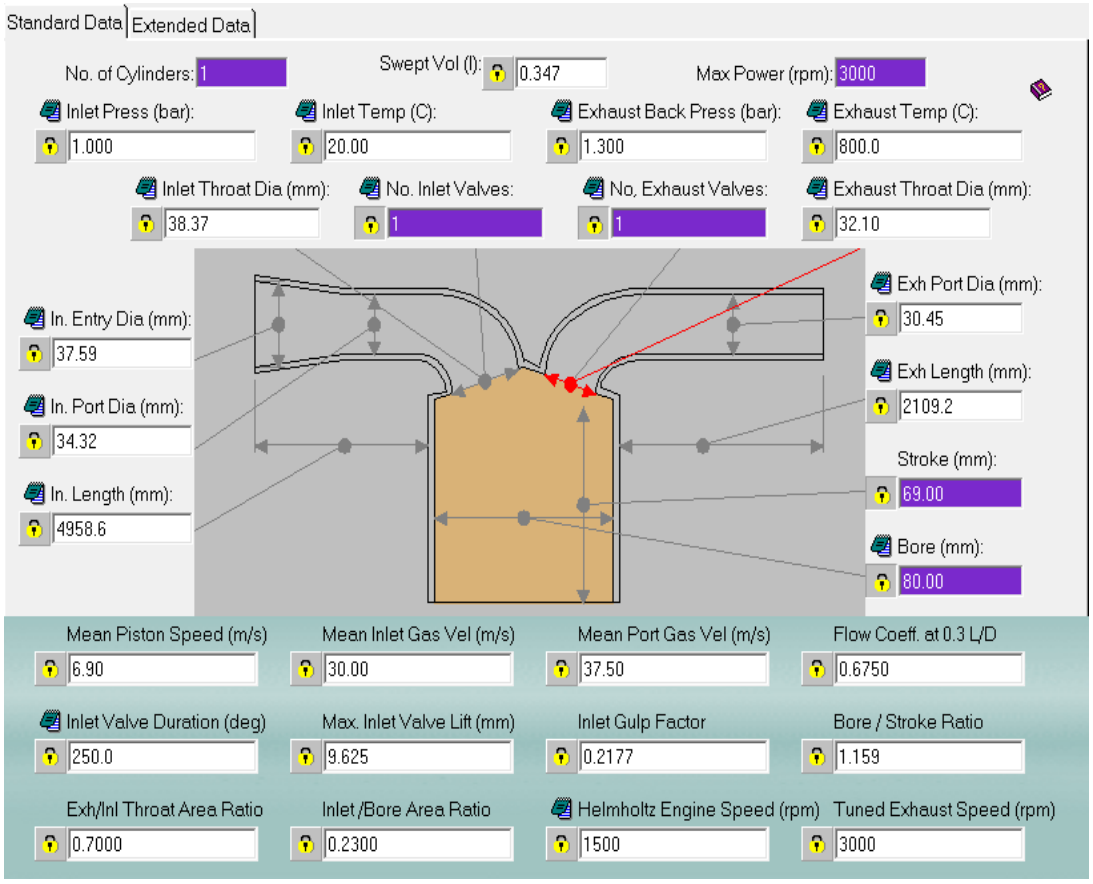

Figure 17 - LES Concept Tool

Since the bore and stroke of the GUNT engine was known, those dimensions were also included in the concept tool. The no. of inlet and exhaust valves was selected to be 1, in accordance with the engine design. Also, since the mean piston speed plays a vital role in connecting rod design, the RPM at max power was selected to be 3000 instead of 3500 in order to achieve the known mean piston speed of 6.9 m/s, and further aid the concept tool to make better predictions. Once these parameters are entered, the LES allows the user to select the intake and exhaust systems for this engine. A common plenum junction

intake and exhaust systems were selected to compliment the single cylinder direct injected design of the engine. It was found that the appropriate connecting rod length for this engine would be 103mm. The concept tool uses the following equations to measure inlet and exhaust throat diameters.

$$D\_in = \sqrt{\frac{0.23}{n_{in}}} \text{ X (bore diameter)} \qquad \text{Equation 7}$$

Where,

D_in is Inlet throat diameter

n_{in} is number of inlet valves

$$D\_exh = \sqrt{\frac{(0.7)D^2 n_{in}}{n_{exh}}} \qquad \text{Equation 8}$$

Where,

D_exh is exhaust throat diameter

n_{exh} is number of exhaust ports

The LES's concept tool creates a schematic of the engine model based on the above mentioned information and transfers it to builder interface of the software. On the builder interface, some more changes were made to tune the engine according to the specifications of the manufacturer. The known compression ratio of 21.5 was selected for the engine and the fuel intake system parameters were changed to direct injected diesel fuel. The intake and exhaust throat diameters calculated by the concept tool were 38.97mm and 66.93mm respectively. But after the initial runs it was found that the

engine provided higher torque than specified by the manufacturer but the volumetric efficiency of the engine was lower. In order to correct this, the intake and exhaust valve throat diameters were changed to 19mm and along with the port valve timings. LES software provides five different valve types as default valve options. The valves in the GUNT engine are controlled by tappets and pushrods, which is very similar to the poppet valve option in the software. Further the dwell time and the valve opening and closing time were tuned to achieve the desired power and torque output. The LES software has two default polynomial lift curves for a popper valve which is fast or slow lift. According to Lotus Engineering, each polynomial is designed to have four coefficients (such that their sum is -1) and their corresponding exponents. A slow lift poppet valve was found to be the most suiting for the GUNT engine in terms of the output.

The LES software allows the users to choose port flow coefficient curves for inlet or exhaust port as well. It gives an option of either poor or good port flow coefficients. These coefficients are a function of valve throat to bore area ratio obtained from the lotus port flow database. They are a ratio of each valve lift and throat diameter (L/D) and are summarized in the form of contour maps as shown in Figure 18 and Figure 19. Every calculated ratio of valve throat to bore area in each simulation is interpolated or extrapolated to either a good or poor port flow characteristic (Copyright Lotus Engineering, 2001). The simulation for GUNT was tried with each option along with an intermediate option of 0.3 L/D and it was noticed that the performance was not affected significantly.

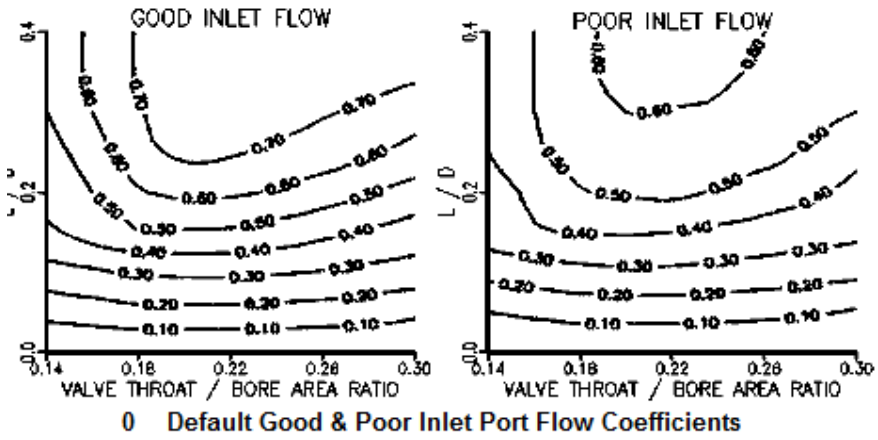

Figure 18 - Inlet Port Flow Coefficient Curves used by LES

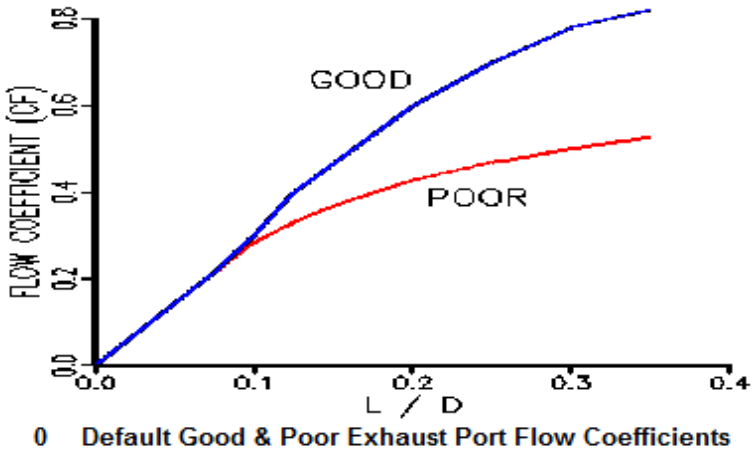

Figure 19 - Exhaust Port Flow Coefficient Curves used by LES

NOTE: No separate port flow analysis was carried out but instead default coefficient calculations from the port flow tool were used.

	Intake	Exhaust
Angle (deg)	10	10
Valve open (deg)	49	76
Valve close (deg)	74	39
MOP (deg)	102.48	-108.52

Table 4 - Intake and Exhaust Port Timings for GUNT Engine (Diesel)

Since this was a single cylinder direct injected engine with one intake and exhaust port, the intake and exhaust plenum volumes were chosen to be the same as the cylinder displacement volume.

- Combustion model

The program is designed such that, the heat released during the combustion is assumed to be heating the whole combustion space. This is because the LES software implements a single zone heat release model. “The main implication of this assumption is that the bulk gas temperature is generally lower than the core combusted gas temperature behind the flame front” (Copyright Lotus Engineering, 2001). Further, Lotus claims that this might have an influence on the detailed in-cylinder heat transfer but, since the theoretical heat models make gross assumptions for heat transfer coefficients and wall temperatures, the discrepancies are minimal. The GUNT combustion model was chosen to be a two part Wiebe function which is more suitable for a direct injected diesel engine. Another benefit of using this function is that it is based on combustion duration and so by manipulating the combustion duration of a specific engine, a more realistic heat release rate can be achieved. The function defines the mass fraction burned in the premixed combustion period as,

$$1 - \left[1 - \left(-\frac{\theta}{\theta_b}\right)^{c_1}\right]^{c_2} \qquad \text{Equation 9}$$

And the mass fraction burned during the diffusion combustion period as,

$$1 - \exp^{-A\left(\frac{\theta-\Delta}{\theta_b-\Delta}\right)^{M+1}}$$ Equation 10

Therefore, m_{frac} = β[pre-mixed] + (1-β)[Diffusion].

Where,

A = A coefficient in Wiebe equation = 6.9

M = M coefficient in the Wiebe equation = 0.4

C1 = “cp1” coefficient in Watson & Pilley equation = 2.0

C2 = “cp2” coefficient in Watson & Pilley equation = 5500

β = fraction of premixed combustion to total combustion = 0.05

Δ = delay angle between premised and diffusion combustion = 0.0

θ = actual burn angle (after start of combustion), and

θ_b = total burn angle (0-100% burn duration) (approx. calculated to be 102.621 degrees).

NOTE: currently there are no defaults available for a two part heat release equations but the values stated above are typical values for the constants in a turbocharged direct injection diesel engine.

- Cylinder Heat Transfer

The heat exchange in the cylinder gases is calculated at each crank angle bases on the wall area, its temperature and the surface heat transfer coefficient. The total cylinder wall area can be calculated using the head and bore dimensions of the engine and the instantaneous liner area is based on the sum of piston clearance and piston location from the TDC at every crank angle. For the wall temperatures, the software assumes certain head flame face thickness (0.13 x Bore) and liner thickness (0.07 x Bore). For the GUNT engine, the head flame face thickness was calculated to be 10.4mm and the liner thickness was 5.6 mm. Some other assumptions made by the LES software are:

- Thermal conductivity of Aluminum as 150 (W/m/K)
- Coolant temperature to be 100^{o} C and its connective heat transfer coefficient as 10000 $W/m^2/K$ for the cylinder head and 8000 $W/m^2/K$ for the liner
- The heat transfer rate of the liner wall temperature is assumed to be 44% of that of cylinder head for convenience
- The cylinder head temperature is calculated as an average of wall temperature and valve temperature.
- piston head temperature as an area averaged cylinder head temperature
- For diesel engines, it assumes the valve temperatures based on the air fuel ratio (AFR)
    - -4.1 AFR + 504.2 ^{o} C (inlet valve)
    - -4.2 AFR + 663.0 ^{o} C (exhaust valve)

LES software provides the three options for in-cylinder heat transfer models in both open and closed period; Annad, Woschni and Eichelberg. All the models generate values

for convective heat transfer coefficient in all the cylinders. For the GUNT engine, Eichelberg heat transfer model was used due to its ease of tuning.

$$h = A \cdot \bar{U}_{\text{piston}}^{-0.33}(p.T)^{B} \qquad \text{Equation 11}$$

Where,

h=heat transfer coefficient

A = Eichelberg open or close cycle A coefficient (2.43)

B = Eichelberg open or close cycle B coefficient (0.50)

$\bar{U}_{\text{Piston}}$ = mean piston speed

p = cylinder pressure

T = cylinder temperature.

Once all the proper adjustments and selections were made, the modeled engine was simulated and the results were tabulated and charted. The finished LES model for the GUNT engine can be seen in Figure 20.

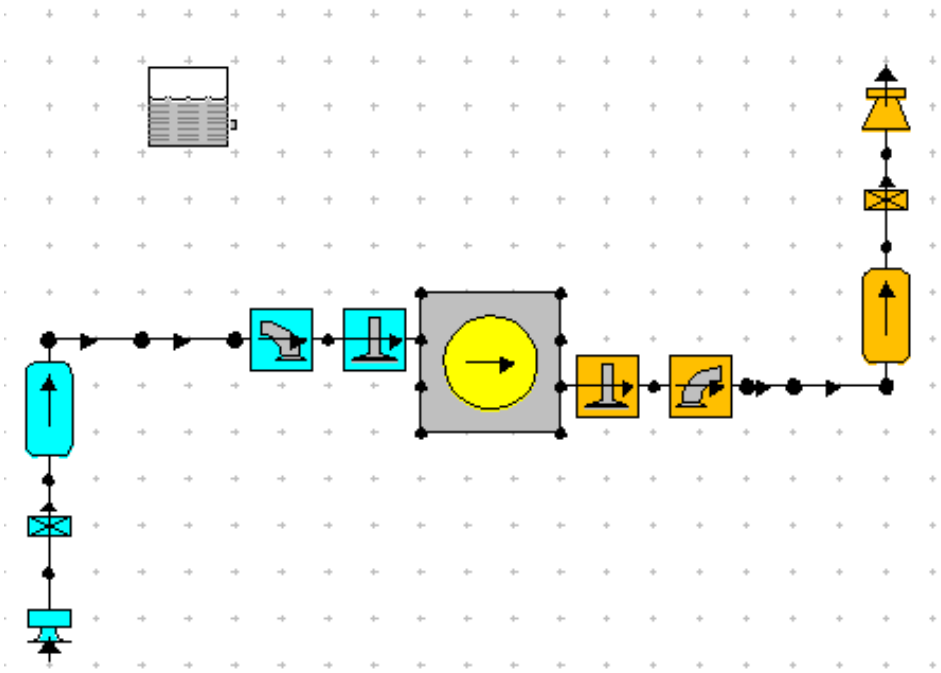

Figure 20 - LES GUNT Model (Diesel)

But before the simulated results can be compared with the dynamometer results and that performance claims of the manufacturer, it was important that the software results are adjusted for the mechanical friction in the engine. The actual GUNT engine is motored by an asynchronous electric motor, manufactured by Alda Antriebstechnik whose mechanical efficiency was found to be 87%. Therefore, the torque results from the software simulation were multiplied by 0.87 so a more realistic data is generated which is adjusted for the motoring losses of the engine. Figure 21 shows the final output results and their comparison.

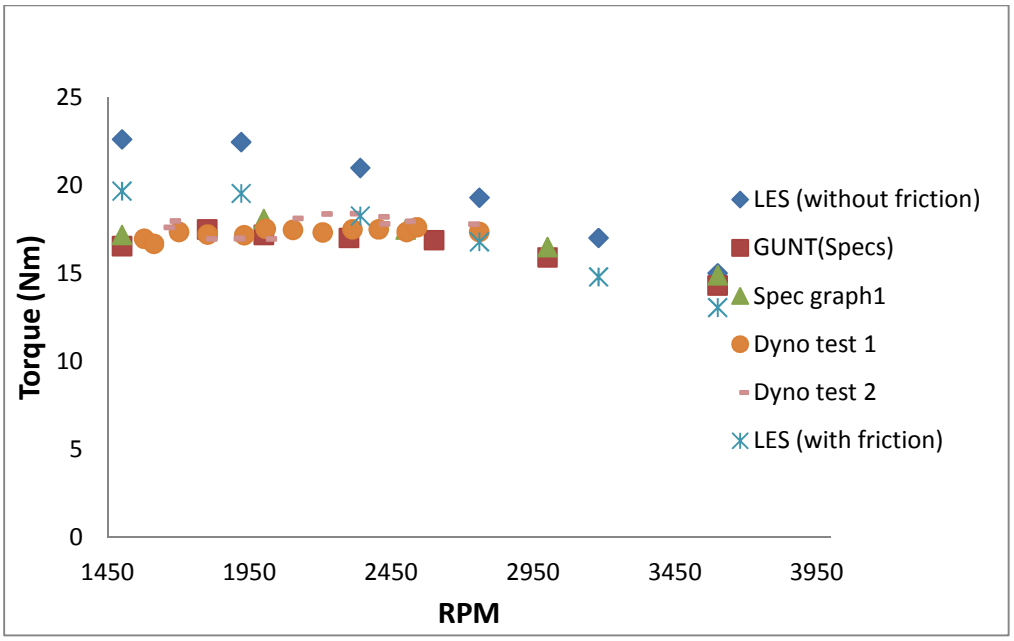

Figure 21 - Comparison of LES Result of the GUNT Engine (Diesel) with Dyno Tests

It can be noticed in Figure 21, that the LES results for output torque are higher without compensating for the mechanical efficiency of the electric motor, whereas the dynamometer torque test results coincide very well with the manufacturer specifications. It can also be noticed that the LES results are slightly optimistic. This is because a perfect displacement scavenging model was selected for the simulation, which assumes that the charge gas entering the cylinder is not mixed with the gas already in the chamber. This means that during exhaust, all the residual gas is removed and only fresh charge of air is present in the chamber during combustion. This is not the case in an actual engine combustion cycle. But the simulation results are very comparable to the test and Specification data, as well as show the same trend in the curve. The results generated by the software are substantially accurate, making the LES a reliable tool to further test and develop the Wiseman engine.

Wiseman LES (Two Stroke)

Once again a similar process was followed in modeling the two stroke Wiseman hypocycloid engine in the LES software. The Wiseman prototype is much simpler in design than the GUNT engine, so modeling it in the LES software was easier. It is a single cylinder spark ignited configuration and the cylinder dimensions like bore, stroke, connecting rod length, compression ratio and displacement volume was provided by WTI. An intake disc valve was used in addition to variable volume inlet plenum. Wiseman engine has piston ported intake and exhaust valves as the engine intake and exhaust. The Wiseman engine runs on gasoline and has a spark ignited carbureted fuel system. The intake and exhaust port on the piston chamber were measured from the actual piston ports of the engine and were found to be as following;

	Intake	Exhaust
Port width (mm)	40	20.82
Max. Port Height (mm)	2	7.41
Valve Open (deg)	124	108

Table 5 - Wiseman LES Port Data

The intake and exhaust pipe geometry was assumed to be simple tubes with approximate dimensions of the carburetor nozzle, at wide open position. A single Wiebe combustion model is used in the modeling of the Wiseman engine since that is more suitable for such engines. According to Lotus engineering, the single Wiebe function defines the mass fraction burned as;

$$1 - \exp^{-A\left(\frac{\theta}{\theta_b}\right)^{M+1}}$$ Equation 12

Where,

The Wiebe coefficients A and M for gasoline are 10.0 and 2.0 respectively.

A more simpler, Annad heat transfer model was used for the Wiseman engine which was given by;

$$\frac{hD}{k} = AR_e^B \qquad \text{Equation 13}$$

Where,

h = heat transfer coefficient

A and B = Annand open or close cycle coefficients

K = thermal conductivity of gas in the cylinder

D = cylinder bore diameter

Re = Reynolds number based on the means piston speed and engine bore.

The A and B coefficients for a carbureted or a port injected combustion system is 0.2 and 0.8 respectively.

Modeling the Hypocycloid Piston Motion

A major assumption the LES software makes is that the engine uses the slider-crank mechanism and so the results calculated are according to the piston motion of a conventional slider-crank mechanism. For the Wiseman engine, the most important aspect of the design was the hypocycloidal piston motion as a result of its unique mechanical assembly. For such special cases, the LES software has a provision to run user specific subroutines while simulating the piston motions during the tests. To find the

equation of the piston motion of the Wiseman engine and the volume above the piston at every crank angle, the following calculations were carried out.

The volume above the piston for a convention slider-crank engine (zero volume at TDC, does not include clearance volume) for a given crank angle can be found using

$$x = a\cos\theta + (l^2 - a^2 - \mathrm{Sin}^2\theta)^{1/2} \qquad \text{Equation 14}$$

$$V = \frac{\pi B^2}{4}(l + a + s) \qquad \text{Equation 15}$$

Where,

x is the piston position, maximum at TDC

a is the crankshaft radius (or stroke divided by 2)

θ is the crank angle with 0º being TDC

l is the length of the connecting rod

V is the volume above the piston, and is equal to 0 at TDC

B is the diameter of the cylinder diameter (bore)

The equations for finding the volume above the Wiseman piston were derived using Figure 22.

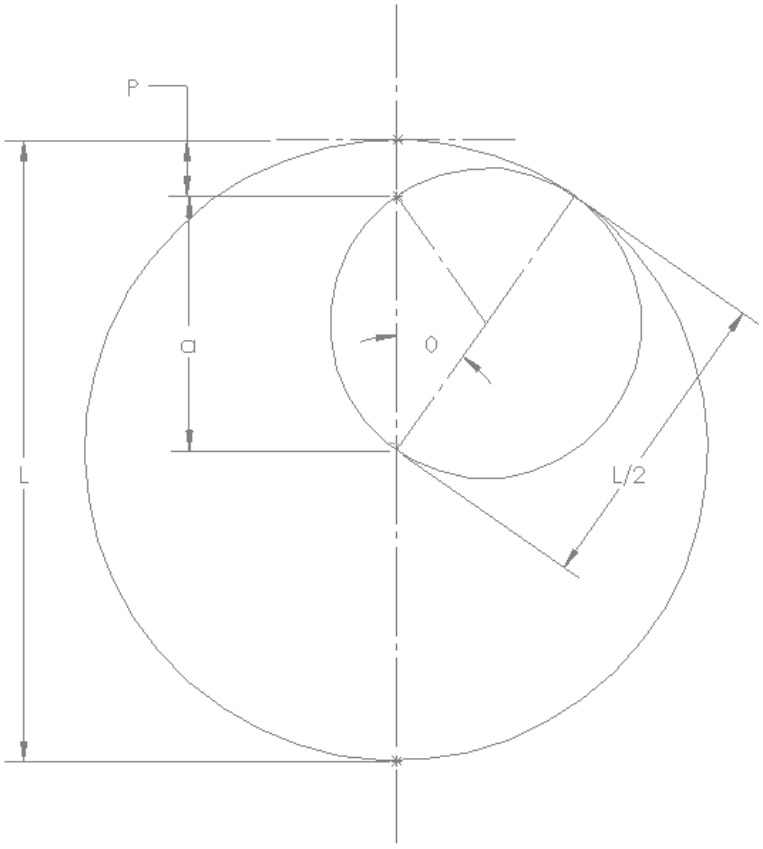

Figure 22 - Wiseman (Hypocycloid) Piston Position Diagram

The distance P or the piston position relative to TDC and the volume above the piston is given by,

$$P = \frac{L}{2} - \left(\frac{L}{2}\cos\theta\right)$$ Equation 16

$$V' = P\left(\frac{\pi B^2}{4}\right)$$ Equation 17

Where,

L is the stroke of the engine.

θ is the crank angle with 0^o being TDC.

V' is the volume above piston, TDC being 0.

B is the diameter of the cylinder (bore)

P is the position of the piston with the origin being TDC.

From previous research it was known the volume of the Wiseman engine at each crank angle is lower than that of the stock engine because its piston sits higher than the stock engine. This provides less combustion volume at each crank angle.

In order to simulate the engine results using the hypocycloid motion, the .DLL file that the software uses to simulate and compile the results was modified. There were subroutines coded within the original .DLL using FORTRAN so switching between the convention slider-crank and the hypocycloid piston motion could be done with ease. The new equations of the piston motions of both the type of engines were changed according to the equations mentioned above.

To verify that the modified code accurately simulated the hypocycloid piston motion, the crank angle, piston speed and position were recorded using virtual sensors attached to the engine cylinder block in LES software. This data was then plotted with respect to time and the difference in curves was studied as seen in Figures 23 and Figure 24. The plots clearly indicate that the modified LES software subroutine simulated engine performance using the hypocycloid piston motion and not a conventional slider-crank piston motion.

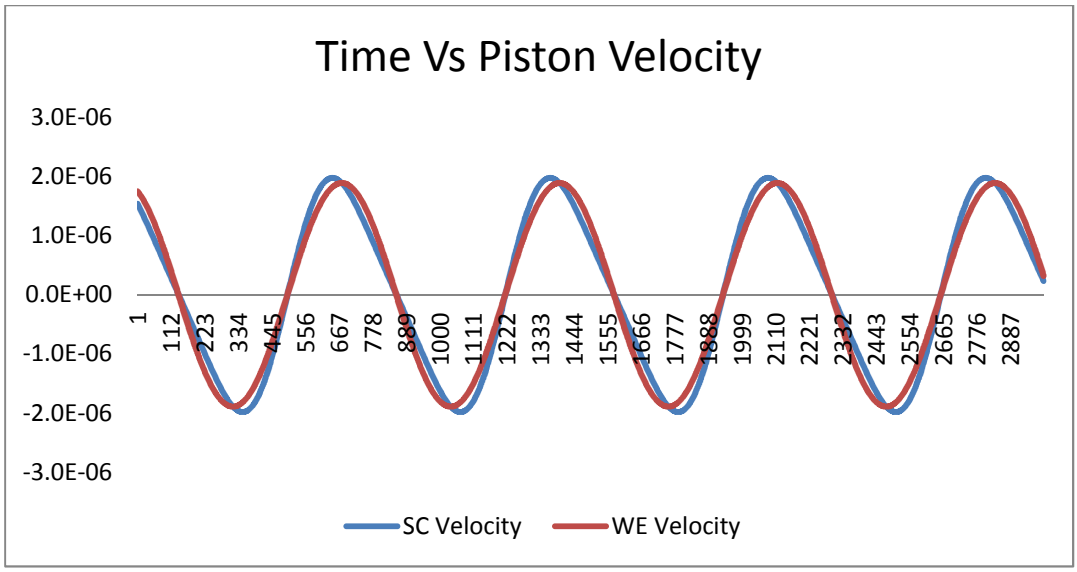

Figure 23 - Comparison of Time Vs Piston Speed of Slider-crank and Wiseman Engine

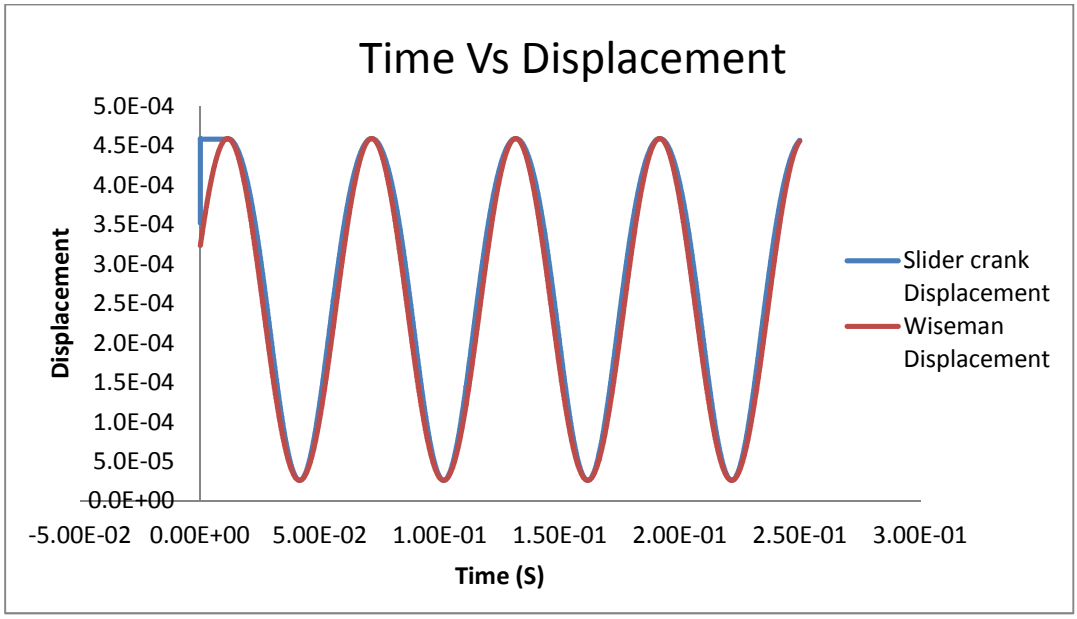

Figure 24 - Comparison of Time Vs Displacement Vol. of Slider-crank and Wiseman Engine

It can be noticed in Figure 24 that the piston motion for a slider-crank engine does not trace a perfect cosine-time curve where as the hypocycloid piston motion syncs perfectly

with the cosine curve. There is nonlinearity in the slider-crank mechanism and so the piston motion is not a harmonic function.

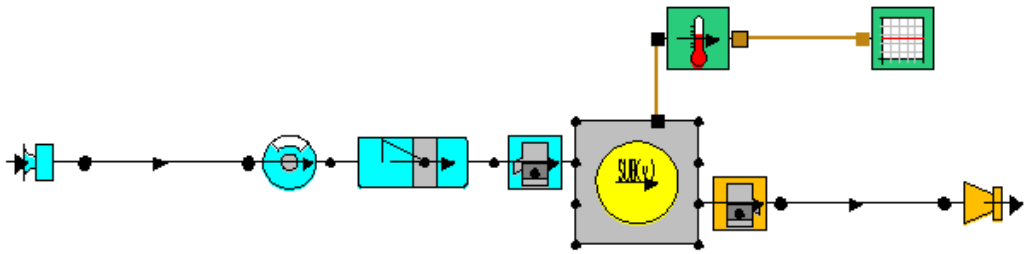

Figure 25 - 2 Stroke Wiseman LES Model

Once the all the required data was entered for each component of the a two stroke model (Figure 25), a speed test was simulated to generate the output data in terms of torque, BSFC and power with respect to the engine RPM. The typical RPM range for a single cylinder spark ignited engine with the size that of Wiseman's is 4500 to 7500 RPM (Ganesan, 2012). Therefore, the model was tested for RPMs ranging from 1000 to 8000. As established earlier, the Wiseman engine has a mechanical efficiency of 0.606 which was also entered for each test point to make sure the simulation at every RPM takes the mechanical efficiency into consideration.

Brake Power and Torque Comparison

During previous research, a dynamometer test was conducted on the Wiseman engine at MTD Southwest Inc. along with a small engine of the same size. The results of that study are summarized in Table 6 (Conner, 2011).

Engine	Peak Power	BSFC
MTD Engine (31 cc)	0.96 HP @ 7000 RPM	410.08 g/hp*hr
Wiseman Engine	0.60 HP @ 6000 RPM	520.06 g/hp*hr

Table 6 - Wiseman Dynamometer Test Summary

From extrapolating the results of the Wiseman engine, they predicted that the engine looses 0.39 HP due to friction. This meant that the Wiseman engine has about 5% higher loss in power than a stock engine of the same size at 7000 RPM.

The software model of the Wiseman engine was simulated using both the piston motion subroutines mentioned earlier. This data was then compared to the dynamometer test results to determine how accurate the LES software predictions are, compared to an actual dynamometer test. The results can be seen on the following plot.

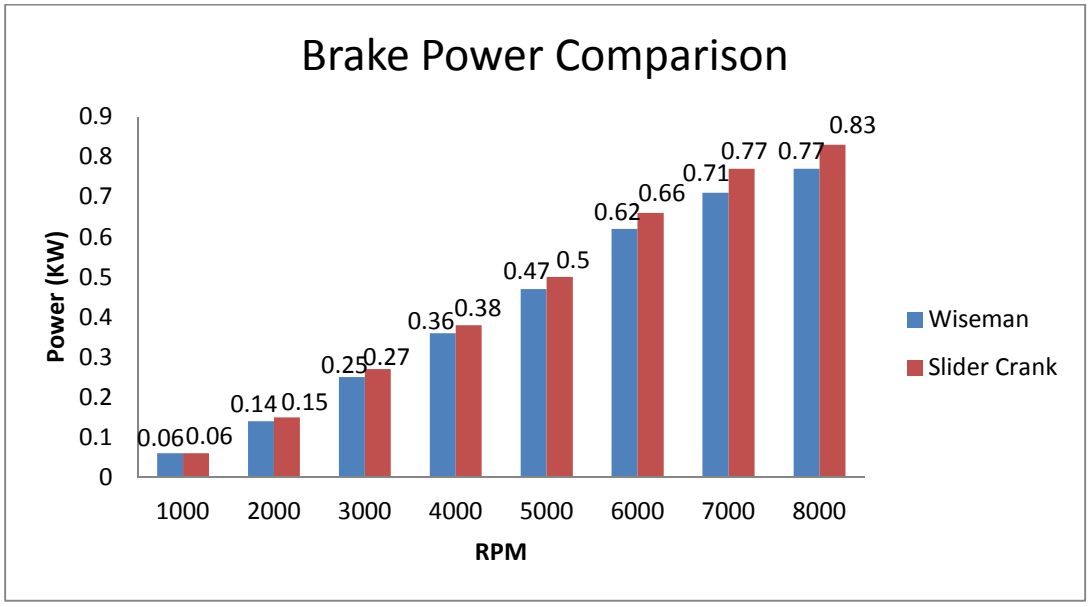

Figure 26 - LES Results of Wiseman and Slider-crank Engine for Brake Power

As seen in Figure 26, the results from the LES software show a very similar trend as the previous dynamometer tests. According to the software results, the Wiseman engine

at 6000 RPM produces slightly less power than the slider-crank engine, which was also the case during the dynamometer test. According to the LES software results, the Wiseman power output at 6000 RPM is 0.62 KW (0.83 HP) and the slider-crank produces 0.66 KW (0.89 HP). The software generated power output at peak RPM of the Wiseman engine is much closer to the theoretically claimed performance of 0.99 HP.

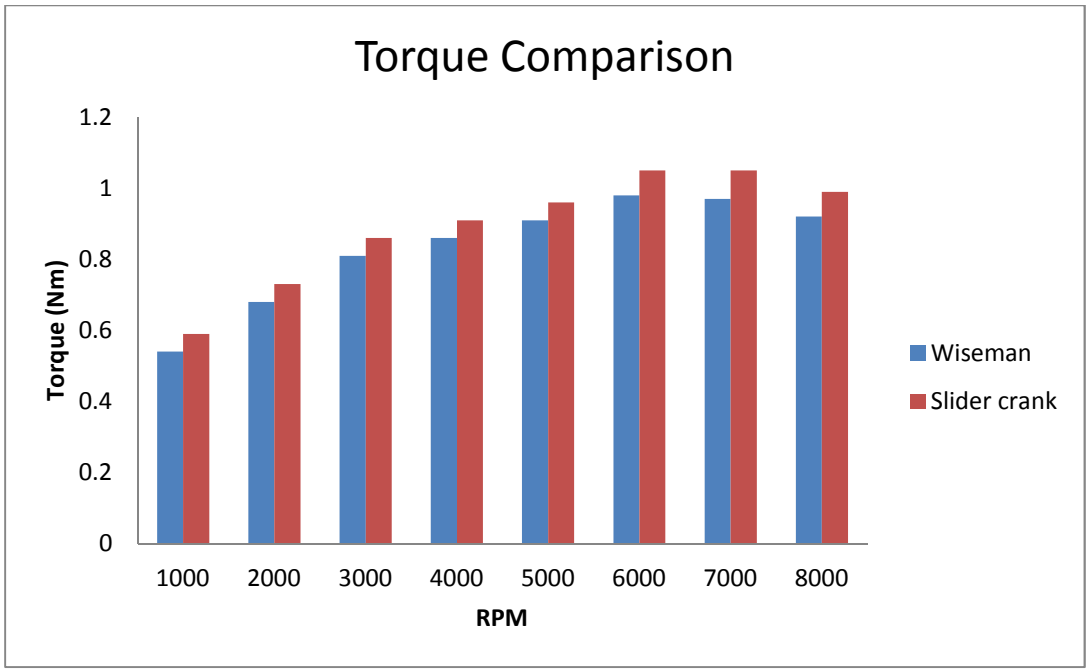

Figure 27 - LES Results of Wiseman and Slider-crank Engine for Torque

Further, comparing the LES results of output torque of the Wiseman engine to that of the conventional slider-crank engine in Figure 27, it can be seen that the torque at peak RPM of Wiseman engine is slightly less than that of the slider-crank engine running at the same speed. Both the engines follow the same trend as the RPM increases. This could be because the Wiseman engine has a longer stroke than that of the slider-crank engine but less combustion volume. The Wiseman engine at 6000 RPM produces 0.98 Nm of torque and the slider-crank produces 1.05 Nm.

Brake Specific Fuel Consumption (BSFC) Comparison

According to the dynamometer tests conducted in the past, the Wiseman engine proved to be 21 % less efficient compared to a slider-crank engine in terms of BSFC at 6000 RPM. As mentioned earlier the Wiseman Inc. claimed that the Wiseman engine showed results of 140 grams/hp*hr in their fuel consumption tests. From the LES results shown in Figure 28, it can be noted that the Wiseman engine at 6000 RPM resulted in a BSFC of 840.42 g/hp*hr and the slider-crank 795.5 g/hp*hr. This shows that the Wiseman engine is about 6% less fuel efficient than the slider-crank engine. The trend in the Wiseman engine having a higher BSFC is still agreeing with the results from the dynamometer tests. BSFC comparison with varying RPM speeds from software results can be seen in the chart below and the Wiseman engine at almost every RPM has higher fuel consumption than the slider-crank engine.

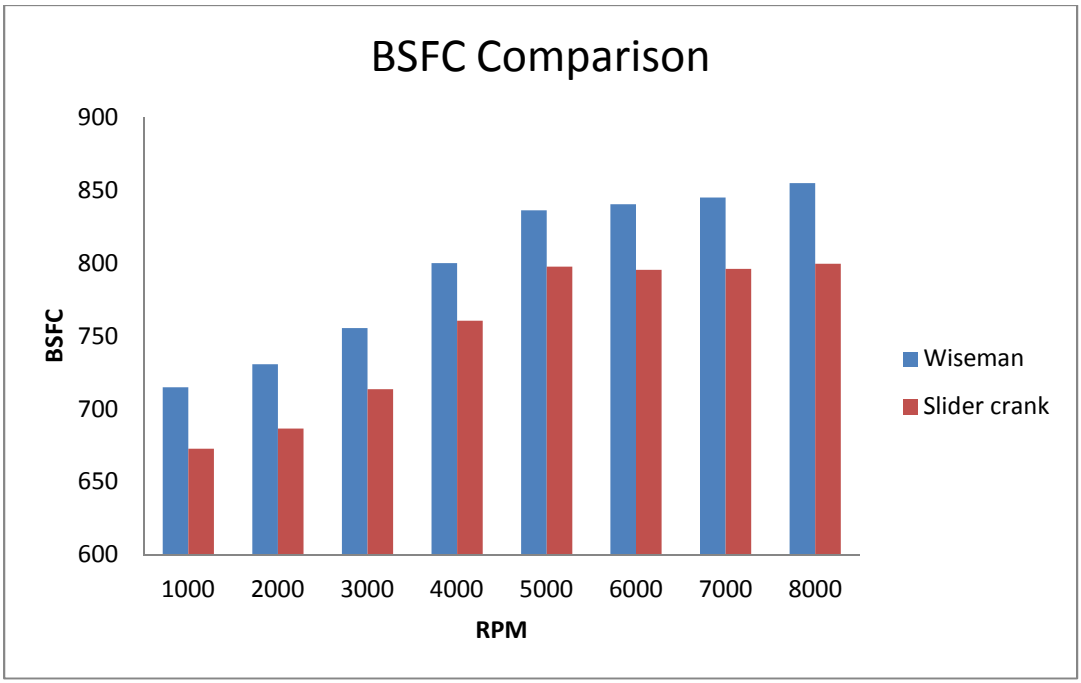

Figure 28 - LES Results of Wiseman and Slider-crank Engine for BSFC

Chapter 5

MULTI-FUEL ANALYSIS OF WISEMAN ENGINE

Considering the choice of combustible fuels available now, it was thought worthwhile to explore multi-fuel variants of the Wiseman engine. A multi-fuel engine is a type of engine that can work on a variety of fuels with insignificant impact on performance and efficiency. There have been slider-crank engines known to run on diesel oil, crude oil, gasoline, JP-4, kerosene, ethanol and even lubricating oil. Such engines have been popular during military operations due to the unpredictable nature of emergencies where no specific fuel type is guaranteed to be available. Diesel engines, due to their high compression ratio, are more compatible to run on a variety of heavy fuels without any major modifications. A properly designed multi-fuel engine has to have good combustion efficiency at different loads and speeds while operating in sub-zero temperatures. It is also required to have low noise, low exhaust smoke and low vibrations, and must not misfire depending on the type of the fuel being used. In order to meet these requirements, some of the design features that a multi-fuel engine needs to incorporate are (Mathur & Sharma, 1997, p. 25):

- High compression ratio to ensure complete combustion of any fuel that it runs on
- Large stroke/bore ratio in order to maintain high temperatures in the combustion chamber
- A reliable fuel delivery system

There are some existing engine types which are suitable as multi-fuel engines but one such engine concept that is of interest to design a multi-fuel variant of the existing Wiseman engine is a variable compression ratio (VCR) engine. Since different fuels have different calorific values, they ignite at different pressures and temperatures. Hence, by providing a feature to change the compression ratio of the engine at which the fuel combusts, the range of fuels that can be used in the engine can be increased.

A VCR engine has primarily seen success in the form of a compression ignited diesel engine rather than a spark ignited engine since the later tends to knock during the lowering of the compression ratio. The change in compression ratio in such engines can be achieved by changing the clearance volume and the swept volume or just the clearance volume alone. A test engine produced by Coordinating Fuel Research Committee, the CFR engine, provides the facility to change the compression ratio by changing the height between the crankshaft axis and the cylinder head (changing the clearance volume). This is done by the means of fine screw-threaded mechanism which allows the cylinder head to be raised or lowered (Mathur & Sharma, 1997, p. 25). A similar design is proposed by the Wiseman Inc., using a contra piston, which will be investigated later in this chapter.

30 cc Wiseman Engine Running on Diesel (Four Stroke)

To begin exploring the performance of the Wiseman engine operating on different fuels, an approach similar to the VCR engine mechanism was undertaken. The existing 30 cc two stroke Wiseman engine was theoretically modified into a 30 cc four stroke diesel engine. This engine was modeled in the LES software and had identical parameters of original Wiseman engine like bore and stroke dimensions, swept volume, and

connecting rod length. The two major changes were the compression ratio, which was changed from 8:1 to 17:1, and the fuel delivery system was changed to direct injection instead of carbureted. This engine was simulated under the same test conditions as the as original gasoline Wiseman engine so the results can be compared with it as well as the slider-crank engine. A comparison of power output, torque and BSFC was carried out for the same RPM range on each engine.

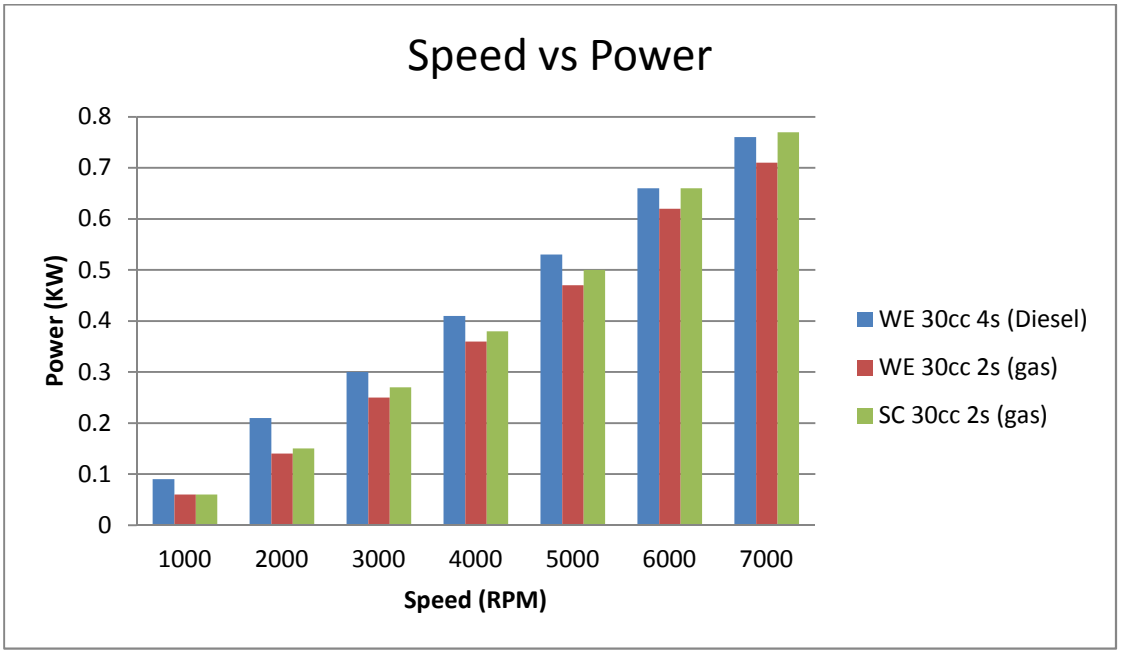

Figure 29 – Power Comparison of Wiseman Diesel, Gas and a Conventional Gas Engines

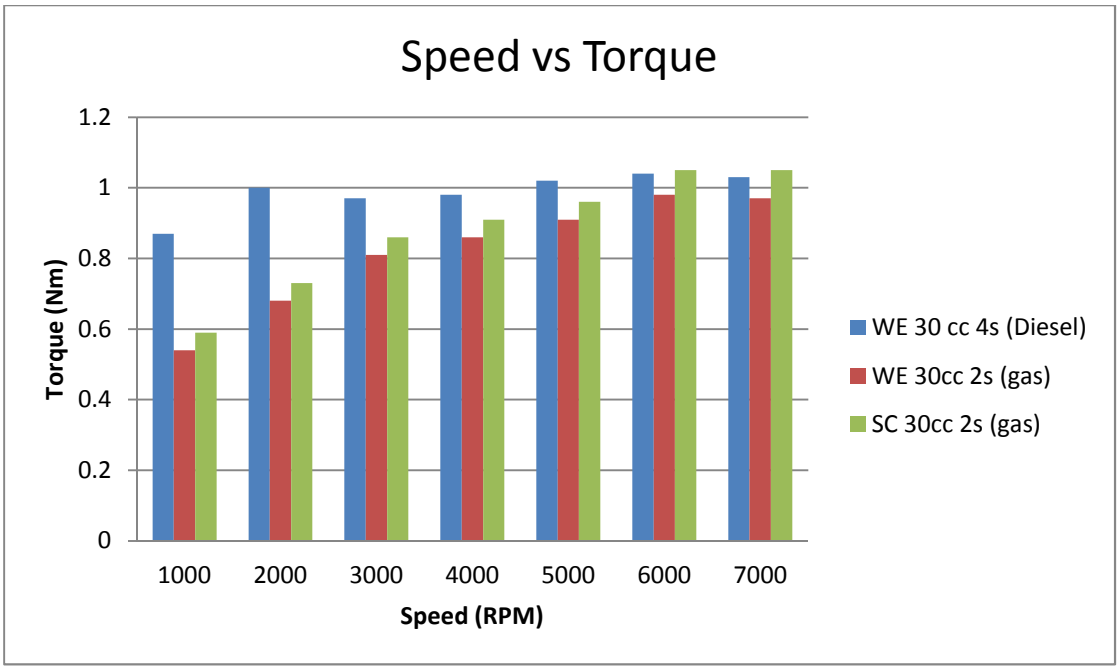

Figure 30 – Torque Comparison of Wiseman Diesel, Gas and Conventional Gas Engines

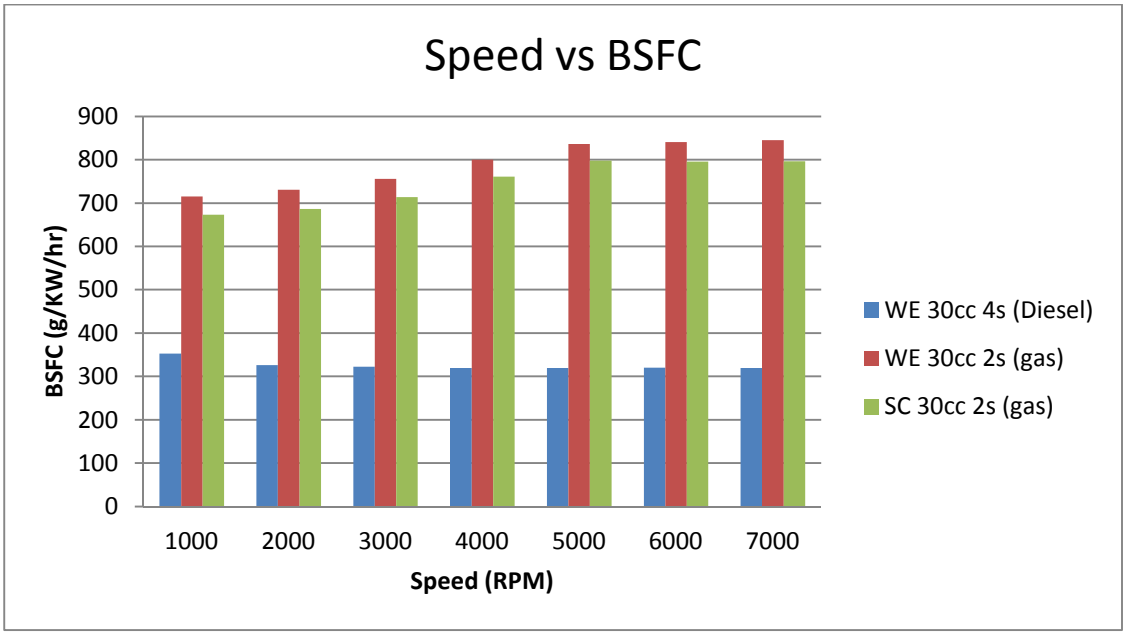

Figure 31 - BSFC Comparison of Wiseman Diesel, Gas and Conventional Gas Engines

From the plotted data, it can be noticed that the Wiseman four stroke diesel engine performs better than the Wiseman two stroke engine (using gasoline) and the

convention two stroke slider-crank engine (using gasoline) in terms of power (Figure 29), torque (Figure 30) and fuel consumption (BSFC) at peak RPMs (Figure 31). The reason for the four stroke diesel engine to perform better than its two stroke counterparts is because a two stroke engine tends to have lower volumetric efficiencies and a part of the fresh air fuel mixture is lost from the exhaust ports. This results in higher fuel consumption in two stroke engines. The proper utilization of the air in the four stroke engine also results in the increased power output. The two stroke engines also have a lower effective compression since some of the piston stroke is lost due to the provision of ports in the combustion chamber (Ganesan, 2012, p. 638).

Engine	Power (KW)	Torque (Nm)	BSFC (g/KW/hr)
Wiseman 2 stroke (gas)	0.71	0.97	845.08
Wiseman 4 stroke (diesel)	0.76	1.03	319.62
Slider-crank 2 stroke (gas)	0.77	1.05	796.2

Table 7 - Performance Summary at the Peak Speed of 7000 RPM

30 cc Wiseman Engine with Contra Piston

The Wiseman engine is known to have more combustion time at the TDC since it follows a linear sinusoidal piston motion which results in increased energy transfer. Due to this, the Wiseman Inc. decided to further enhance the engine platform by announcing a variable compression Wiseman UAV engine (referred to as the Wiseman UAV engine from here on). They propose using an adjustable contra piston which is incorporated in the existing combustion chamber, hence making the bottom face of the contra piston as the top of the combustion chamber. The proposed design has a modified cylinder head with a bolt on top (Figure 32 (c)) to control the distance travelled by the contra piston in

the cylinder, thus changing the clearance volume and the compression ratio. This allows the compression ratio to be changed while the engine is operating. Other then this specific modification the rest of the engine utilizes the existing Wiseman mechanism. This allows to conveniently replace the contra piston (combustion chamber) according to the type of fuel without having to change the entire engine.

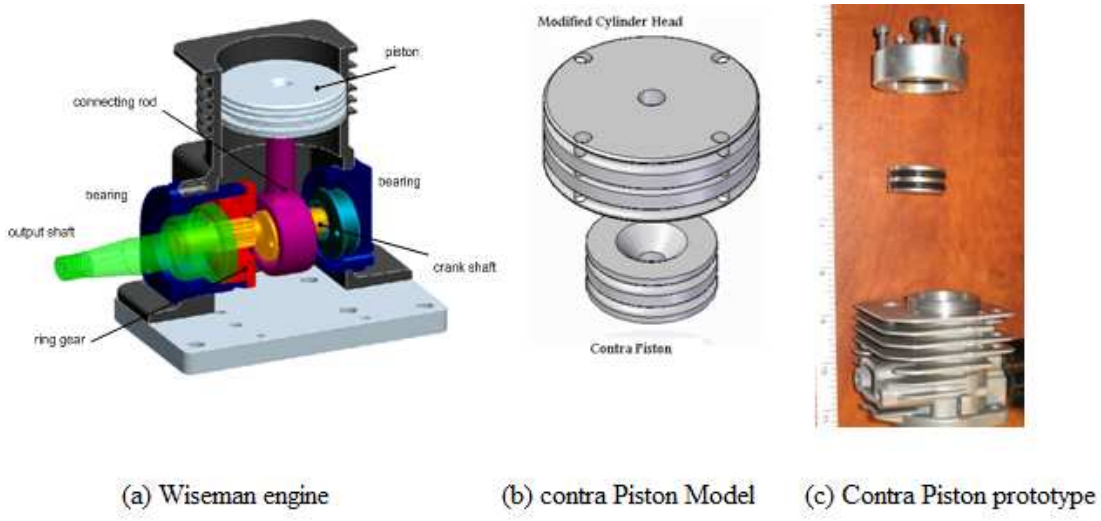

(a) Wiseman engine (b) contra Piston Model (c) Contra Piston prototype

Figure 32 - Variable Compression Wiseman UAV Engine (Wiseman Inc.)

Theoretically it is predicted that, by starting the engine at a low compression ratio (say 9:1) along with a glow plug and then increasing the compression (say 18:1) would result in about 30% increase in power and efficiency (Wiseman Technology, Inc.).

30 cc Wiseman Engine with Contra Piston Running on Ethanol (Two Stroke)

The government of the United States has mandated the use of ethanol-gasoline fuel blend (E10) in ten states. E10 is about 10% ethanol and 90% unleaded gasoline and almost all new automobile engines are designed to run on it. The automakers now cover the use of E10 under their warranty since about 75% of the gasoline in America is now

blended with ethanol. Another popular fuel blend is E85, which consists of 85% ethanol and 15% gasoline. This blend is also known as flex-fuel and many new engines are now being designed to operate on E85. It has a higher octane rating than gasoline and is believed to produce more power. Ethanol when used as a fuel is known to have an anti-knock performance by allowing the engine to run at a higher compression ratios as compared to pure gasoline engines. Though, the ethanol engines tend to have a higher BSFC since it has a lower calorific value than gasoline. This means the engine running on ethanol consumes more fuel as compared to gasoline, to generate the same amount of power and torque output (Costa & Sodre, 2010).

To further analyze the performance of the Wiseman UAV engine using a contra piston, the software model of the current two stroke Wiseman engine was modified accordingly and simulated. To test the performance of the engine while operating on ethanol, the properties of E85 were considered. The only changes made to the engine model were the fuel properties and the compression ratio. Studies show that SI engines running on ethanol blend tend to perform better at a compression ratio of about 12:1 (Costa & Sodre, 2010). All other engine parameters in the LES software model were kept the same as the original, to determine how the Wiseman UAV engine with contra piston would perform in case only the compression ratio was changed with respect to the fuel type.

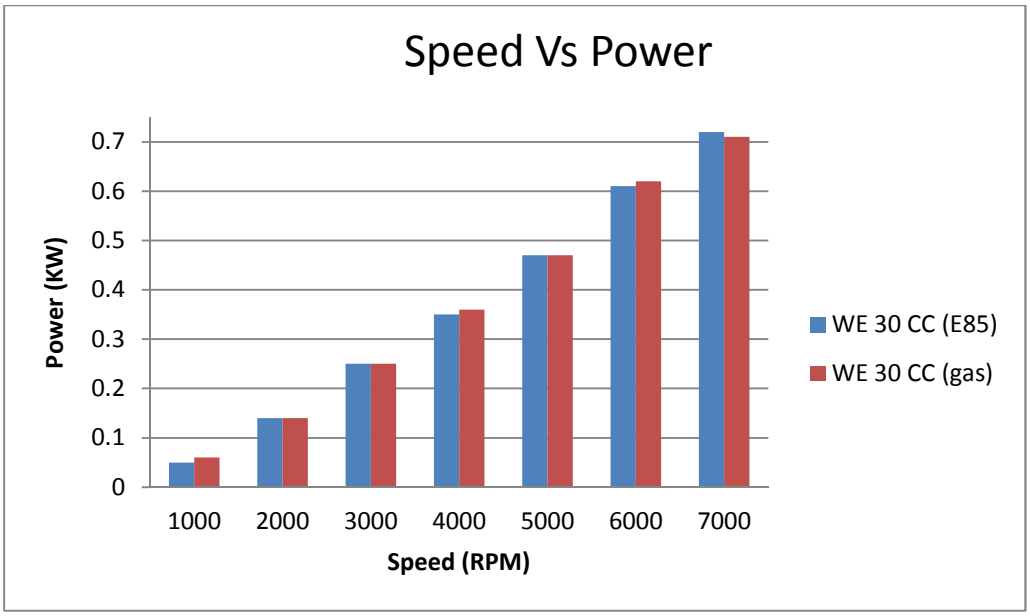

Figure 33 - Power Comparison of Wiseman Engine with Contra Piston (E85 and Gas)

A study conducted on the effects of ethanol in a port-injected gasoline engine showed that the engine produced more power at the speeds above 3000 RPM (Cahyono & Bakar, 2010). An increase of about 5% in output power can be achieved by adding 10% ethanol blend in a spark ignited combustion engine (Datta, Chowdhuri & Mandal, 2012). By increasing the concentration of the ethanol in the fuel blend also tends to increase the overall efficiency, resulting in increased output power (Celik, 2007). A similar trend can be seen in the Wiseman UAV engine results operating on E85. As seen in Figure 33, the engine produces less or identical power when running on E85 in comparison to pure gasoline at lower RPMs, but at the peak RPM of 7000 the output power of the engine running on E85 is 1.4% more than gasoline.

Another reason for higher power output while operating on E85 is because ethanol is resistant to knock, allowing the engine to run on a higher compression ratio, which results in increased cylinder BMEP (Celik, 2007). Also, at higher temperatures,

ethanol has a better thermal efficiency than gasoline since it has a higher heat of vaporization. This means that when the compression ratio is increased, it burns a richer mixture of air-fuel compared to gasoline, resulting in a higher output power (Costa & Sodre, 2010).

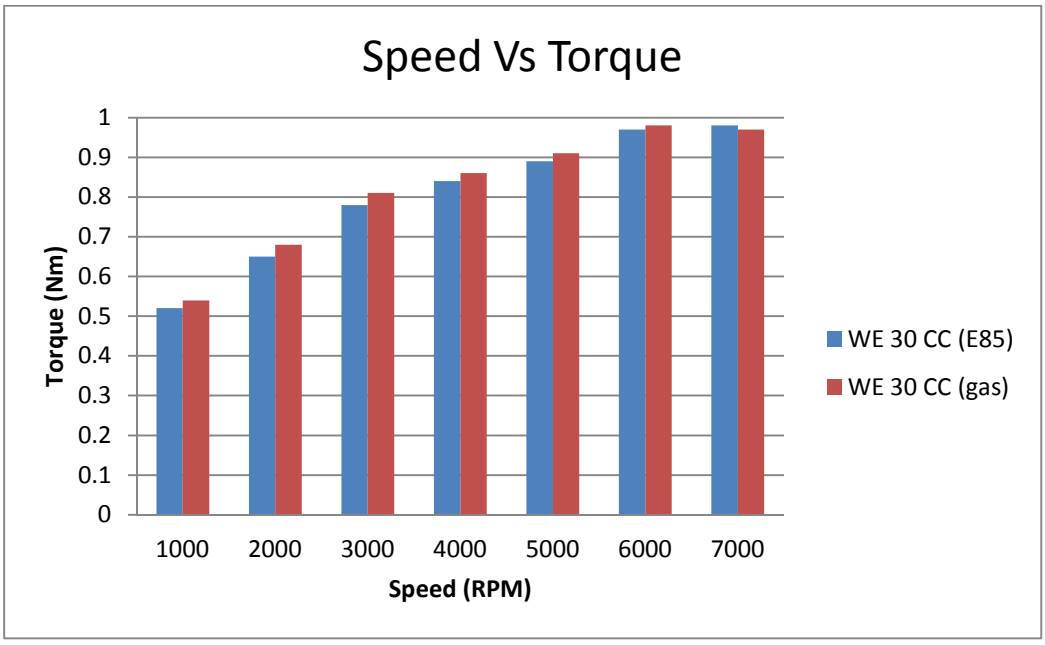

Figure 34 - Torque Comparison of Wiseman Engine with Contra Piston (E85 and Gas)

As seen in Figure 34, the comparison of torque generated by the Wiseman UAV engine while operating on E85 and gasoline shows that the engine produces slightly more torque when operating on E85. The reason behind this is that when the engine is running on E85, it prepares a rich air-fuel mixture increasing the air-fuel equivalence ratio. This means that the fuel burns closer to stoichiometric causing a better combustion (Topgul, Yucesu, Cinar & Koca, 2006). Though, from the simulated results it was noticed that the increase in torque was only achieved at the peak RPM and the difference was not significant. This is because at lower RPMs, the high calorific value of gasoline results in

higher torque but when the speeds increase ethanol blends tends to produce more torque due to its faster flame velocity. Again, the higher compression ratio and cylinder BMEP for E85 engines means more work is done on the piston causing an increase in the output torque (Costa & Sodre, 2010).

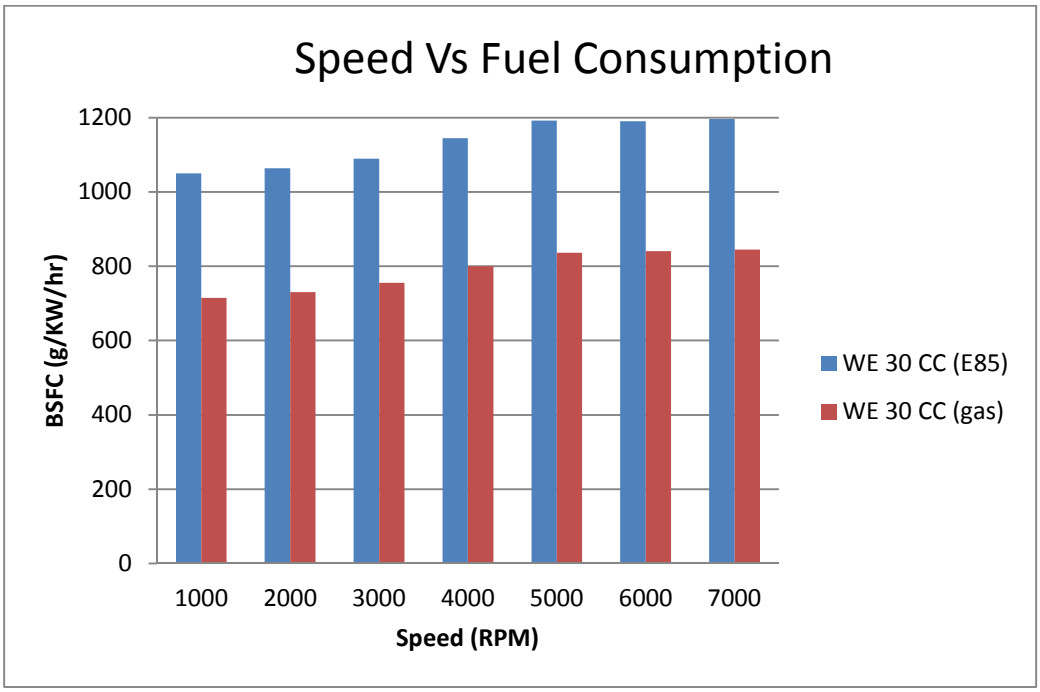

Figure 35 - BSFC Comparison of Wiseman Engine with Contra Piston (E85 and Gas)

Studies show that by increasing the concentration of ethanol by 10-20% in an ethanol-gasoline blend reduces the calorific value of the fuel which causes an increase in the fuel consumption of the engine (Cahyono & Bakar, 2010). As mentioned earlier, ethanol has a significantly lower calorific value as compared to gasoline, which results is lower energy released on combustion. Therefore more fuel is required for an engine running on E85 to do the same amount of work as an engine running on pure gasoline. This trend in fuel efficiency is very evident in the results generated by the LES software. The plotted results in Figure 35 show that the Wiseman UAV engine when running on

E85 tends to consume more fuel at every speed with an increase of almost 41.5% at the peak RPM.

Engine	Power (KW)	Torque (Nm)	BSFC (g/KW/hr)
Wiseman UAV (gas)	0.71	0.97	845.08
Wiseman UAV (E85)	0.72	0.98	1196.21

Table 8 - Performance Summary of Wiseman with Contra Piston (E85 and Gas) at 7000 RPM

Scalability Analysis on Bigger Wiseman Engine Prototypes

To further expand the range of applications utilizing the Wiseman engine, a series of theoretical Wiseman prototypes were designed and their performance was simulated in the LES software (using the conventional slider-crank piston motion and the Wiseman hypocycloid piston motion). The current 30 cc Wiseman engine is designed to produce 0.99 Hp. The theoretical prototypes were designed with the engine output power in mind, and so models for a 10 Hp, 20 Hp and 30 Hp (7.46 KW, 14.91 KW and 22.37 KW respectively) were considered. Another reason for designing Wiseman engine prototypes with higher power outputs was so that, a scalability analysis can be conducted to determine how the engine's performance varies with respect to its size. These prototypes were also tested to predict their performance while operating on different fuels (gasoline, diesel and E85).

The engines were designed to have the following characteristics:

- Single cylinder with a four stroke combustion cycle and a peak performance speed of 2000 RPM
- Compression ratio of 8:1 was chosen for the gasoline engines, 16:1 for diesel engines and 13:1 for Ethanol engines

- Indicated Mean Effective Pressure (IMEP) of 0.7 MPa (Kale, table 3.2)
- Mechanical efficiency (η_{mech}) of 80% (Kale, table 3.5)
- BMEP of 0.56 MPa (IMEP x η_{mech})
- Bore/stroke ratio (L/D) of 1.2 for gasoline and Ethanol engines, and 1.25 for diesel engines (Kale, table 4.16)
- The gasoline and Ethanol engines used a carburetor, and the diesel engines were direct injected.

The following steps further explain the calculations carried out during the designing process of each prototype:

i. Taking the above mentioned characteristics into consideration the engine bore diameter was calculated by,

$$Bp = BMEP \times L \times A \times N \qquad \text{Equation 18}$$

Where,

Bp = Brake horsepower in Watts

BMEP = Brake mean effective pressure

L = Stroke length (1.2 x D)

A = Area of the bore ($\frac{\pi}{4}D^2$)

N = Engine Speed ($\frac{RPM}{2}$)

This step was carried out to calculate the bore diameter for each engine from which their respective stroke lengths were also found.

ii. Once the bore diameter and the stroke length was found, the engine swept volume was calculated using,

$$V_s = A \times L \qquad \text{Equation 19}$$

Where,

V_s = cylinder swept volume

A = Area of the bore ($\frac{\pi}{4}D^2$)

L = Stroke length

iii. Finally, torque at peak performance RPM for each engine was calculated;

$$T = \frac{HP \times 5252}{Speed} \qquad \text{Equation 20}$$

Engine power (KW)	**Bore Diameter (mm)**	**Stroke Length (mm)**	**Swept Volume (liters)**	**Calculated Torque (Nm)**	**Bore to Stroke ratio**	**Swept Volume (cc)**
7.46	94.7	113.64	0.800	35.6	0.83333	800
14.914	119	142.8	1.587	71.21	0.83333	1587
22.371	135	168	2.404	106	0.80357	2404

Table 9 - Calculated Specifications of 10, 20, and 30 HP Gasoline Engines

Engine power (KW)	**Bore Diameter (mm)**	**Stroke Length (mm)**	**Swept Volume (liters)**	**Calculated Torque (Nm)**	**Bore to Stroke ratio**	**Swept Volume (cc)**
7.46	93.4	116.75	0.7995	35.6	0.800	799.5
14.914	117.65	147.063	1.598	71.21	0.7999	1598
22.371	134.68	168.35	2.397	106	0.8	2397

Table 10 - Calculated Specifications of 10, 20, and 30 HP Diesel Engines

NOTE: A similar approach as the Wiseman UAV contra piston engine was used to determine the performance of the gasoline engine running on E85. This meant that the engine parameters for the ethanol engine remained the same as the gasoline engine but the compression ratio was changed to 13:1, and the fuel properties were changed to that of E85.

Scaling Laws for Internal Combustion Engines

Further, to analyze and predict the performance of the Wiseman prototypes with increasing horsepower, there was a need to establish some performance scaling laws to determine how the engine performance changes according to the size of the engine. Every engine's output vary over its operating range, and so comparing their performance at randomly selected points would not draw any meaningful conclusions. In order to compare the output performance metrics across different engines, the engines need to be compared at constant speed (2000 RPM) and air-fuel ratio. This way the changes in the performance can be isolated and treated as a result of change in engine size. Mr. Shyam Kumar Menon has done some extensive work during his master's and doctorate studies on scaling the engine's performance based on the engine size. He studied over 40 engines ranging from single cylinder to 36 cylinders in size. These engines had applications ranging from model airplanes, to lawnmowers, to automobiles and aircrafts (Menon, 2006). Based on the plethora of data that he collected from testing and manufacturers, he established some scaling laws for the engine's performance parameters based on their displacement. These established laws are used to analyze the Wiseman prototypes and determine the effects of scaling them bigger.

I. Scaling the Bore and Stroke of the Engine

There was a relationship established between the engine displacement and the corresponding bore to stroke ratio. It was noticed that the engines with displacement less than 1000 cc were likely to have a “square” design with a few exceptions between the ranges of 1000-8000 cc. This meant that the bore to stroke ratio in those engines was close to 1. Another observation was that, as the engines got larger, the design changed to slightly “under square” (Menon, 2010).

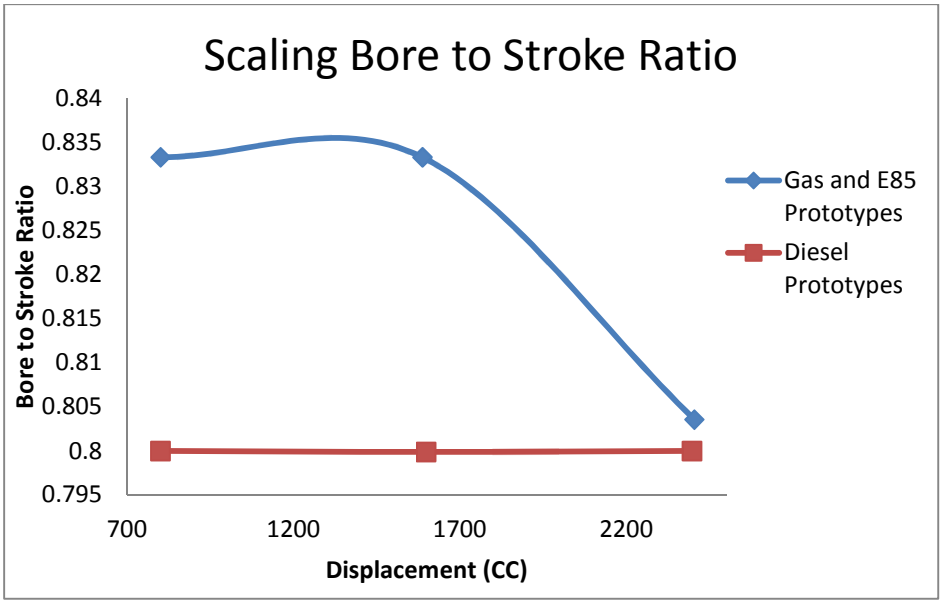

Figure 36 - Scaled Relationship between Engine Sizes and Bore to Stroke Ratio

From studying the calculated displacements of the 10, 20 and 30 HP Wiseman prototypes (gasoline, E85 and diesel) and their corresponding bore to stroke ratios, it seemed that the engines tend to have a bore to stroke ratio closer to 1 regardless of their displacement. This is especially true for the diesel prototypes, as seen in Figure 36. Though, the data set used to test the scaling laws on engine’s physical properties is too small to draw any meaningful conclusion.

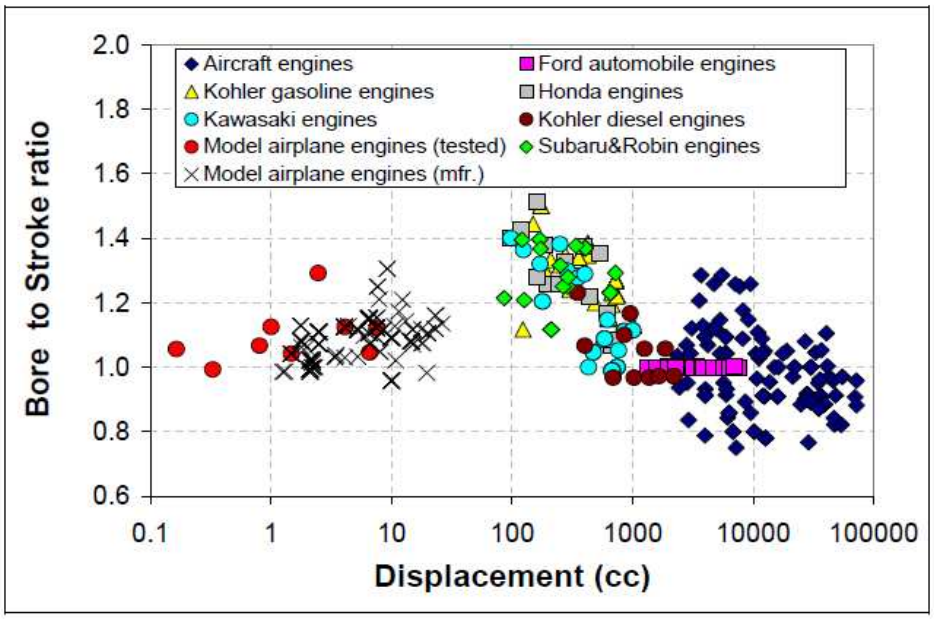

Figure 37 - Scaling of Bore to Stroke Ratio with Engine Displacement (Menon, 2010)

But from studying the data presented by Mr. Menon in Figure 37, it can be noticed that the Kohler diesel engines as well as the Ford automobile engines that he tested showed a similar trend as the Wiseman diesel prototypes between the sizes of 700 to 3000 cc (approximately).

II. Scaling the Engine Peak Torque at Peak Power Output

Further, two different power laws were established by Mr. Menon, one for the small engines he tested and another based on the manufacturer provided data. But since both the laws had a close correlation ($R^2 > 0.98$), it was concluded that the output torque as a function of displacement can be described using a power curve, regardless of the size and type. It was noted that the engine torque tends to increase with the increase in the engine displacement. A chart projecting the data collected by Mr. Menon can be seen in Figure 38.

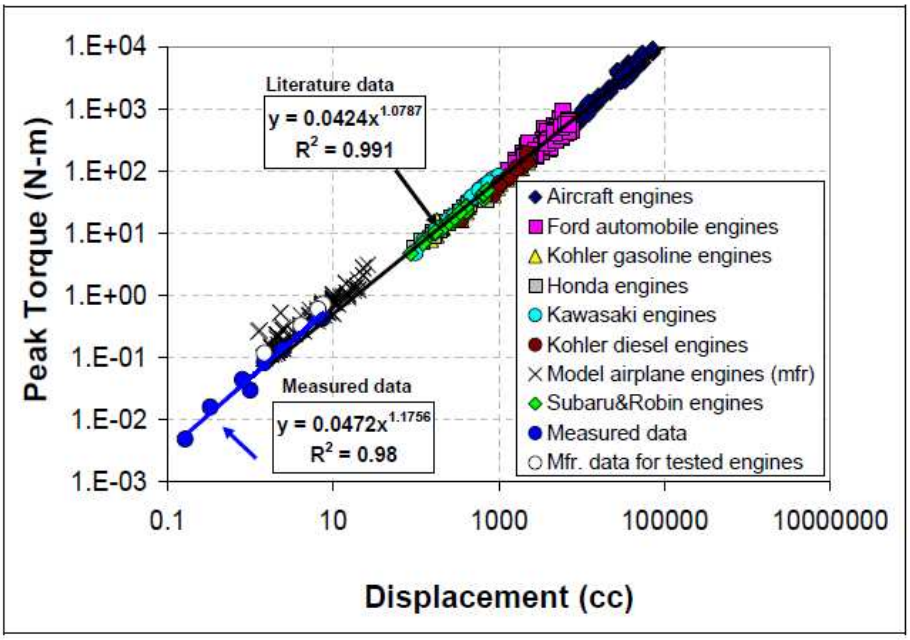

Figure 38 - Scaling of Peak Engine Torque with Engine Displacement (Menon, 2010)

The data generated from software simulations of each engine type was then plotted to see how close the fit was when compared to the above mentioned relationship.

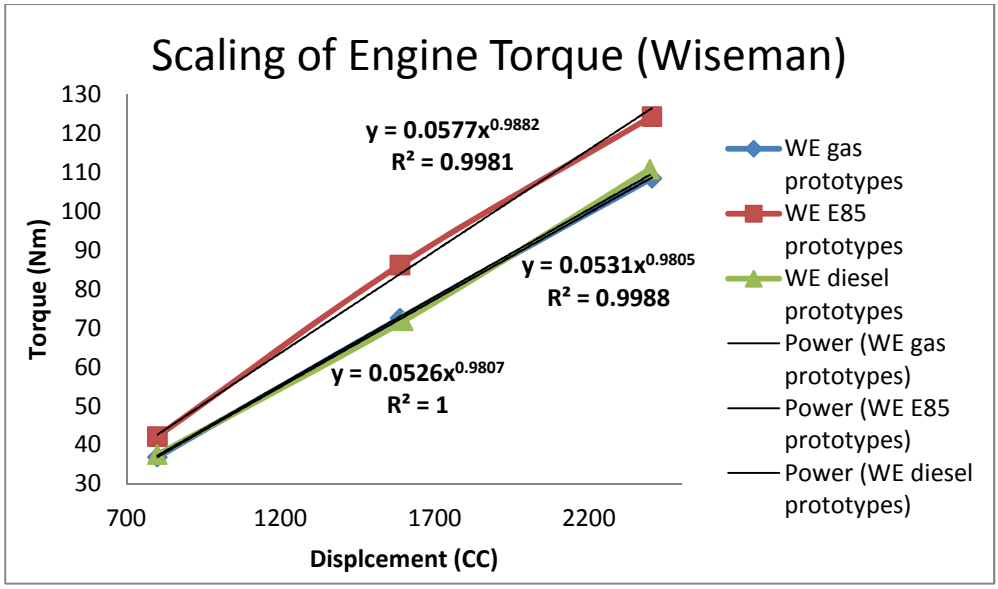

Figure 39 - Scaling Wiseman Engine's Torque with Engine Size at 2000 RPM

As seen in Figure 39, the Wiseman engines follow a similar trend when the displacement and the corresponding output torque of the engines are compared. The correlation of the power curves is R^2 >0.99 and the torque seems to be directly proportional to the displacement. This means that as the Wiseman engine's size in terms of cylinder displacement increases, the output toque also increases. This is true for E85, gasoline and diesel engines.

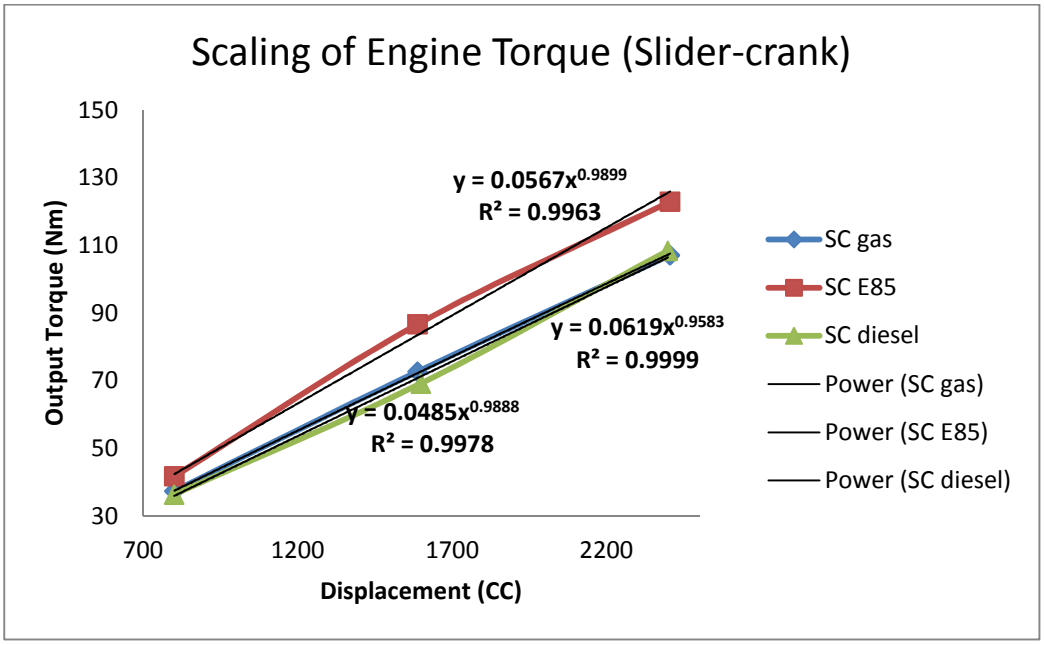

Figure 40 - Scaling Slider-crank Engine's Torque with Engine Size at 2000 RPM

Once again, from Figure 40, it can be noticed that the output torque for the slider-crank engines of the same size as the Wiseman prototypes, while operating on E85, gasoline and diesel, also show a very similar trend to the scaling law established by Mr. Menon.

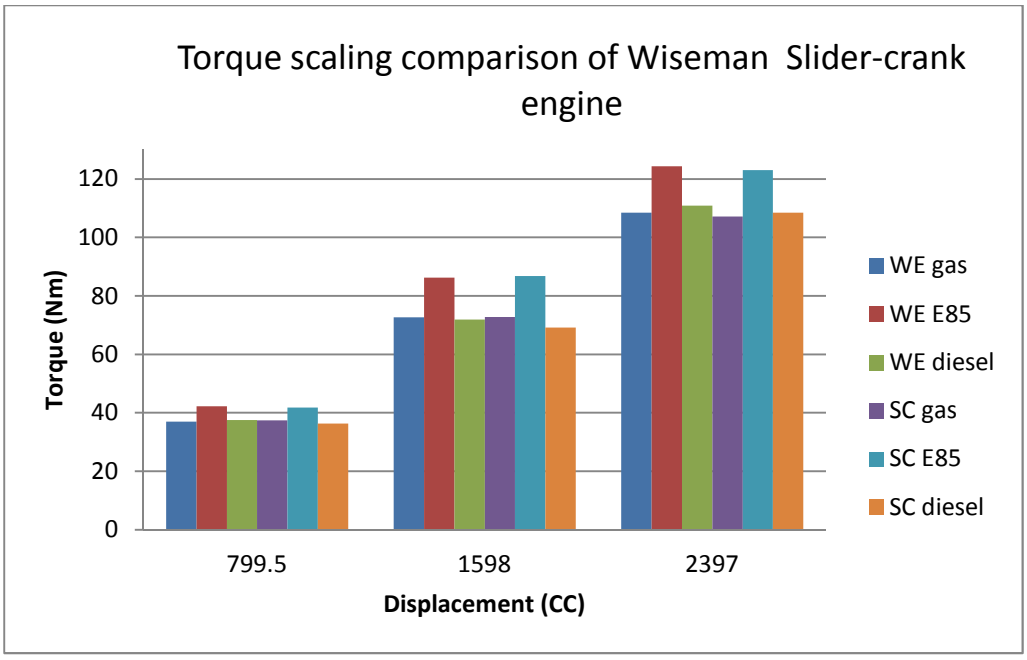

Figure 41 - Comparing the Scaled Torque of Wiseman and Slider-crank Engine

Figure 41 shows a comparison of the output torque of the Wiseman engines and slider-crank engines of the same size while operating on different fuels. It can be seen that as the engine displacement increases, the Wiseman variants tends to produce slightly more torque than the slider-crank engines of the same size. But the difference does not seem to be of a significant margin. The Wiseman engine is known to produce lower torque compared to a slider-crank engine of the same size at lower engine displacements because of its shorter stroke length. But eventually this is compensated due to its lowered cylinder friction.

III. Scaling the Engine Peak Power Output

A similar trend was also noticed in the peak power output when compared to the engine's size. This meant that the engine output power increased as the engine

displacement increased. But during his research, Mr. Menon noticed that the change in the output power for a two stroke engine was more than that for a four stroke engine of the same displacement (shown in Figure 42). This makes sense since it is a well known fact that two stroke engines tend to produce more power per unit displacement (Menon, 2010).

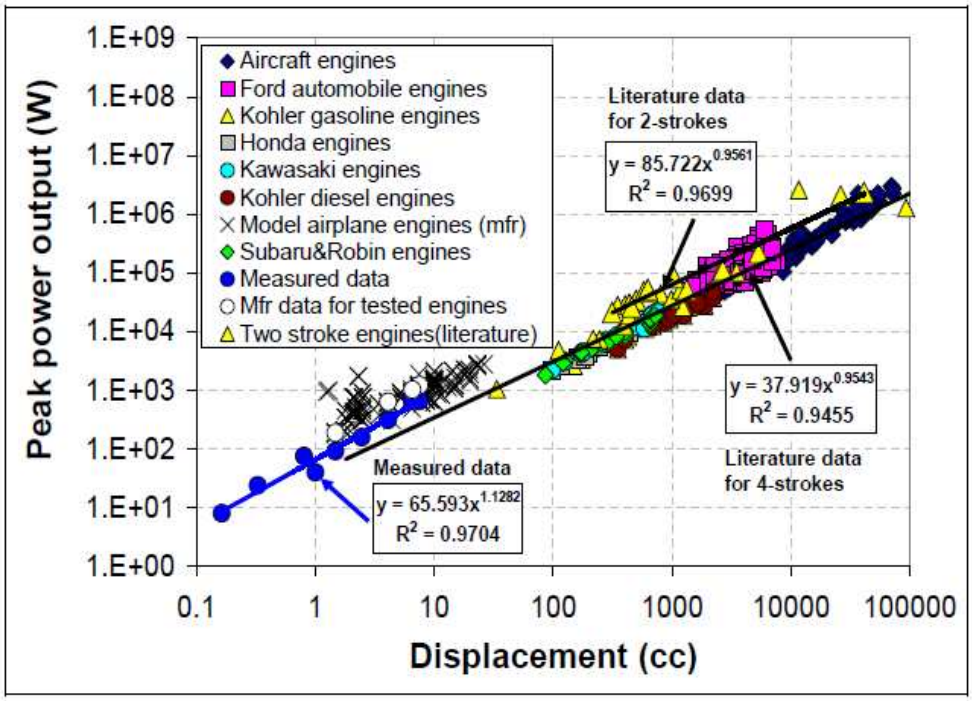

` Figure 42 - Scaling Peak Engine Power Output with Engine Size (Menon, 2010)

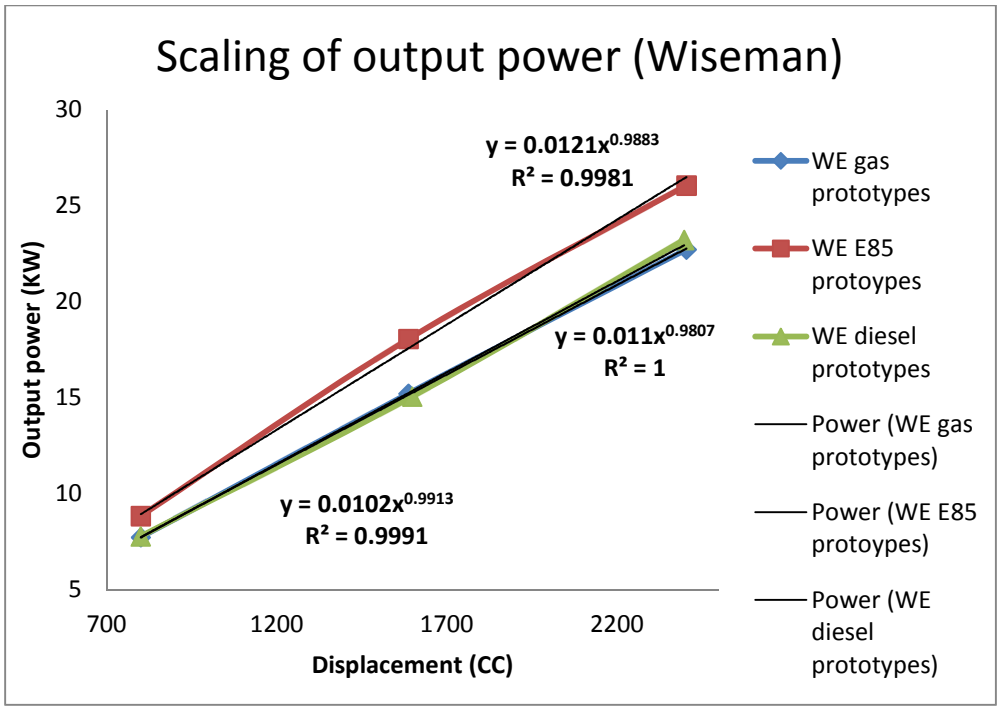

Figure 43 - Scaling Wiseman Engine's Peak Power with Size at 2000 RPM

Once again, from Figure 43, it can be seen that the output power of the engine as a function of the engine displacement tends to follow a similar trend as the output torque. The Wiseman prototypes tend to have an increased output power as the displacement of the engine increases, irrespective of the fuel type. Figure 44 suggests that this is also true for the slider-crank engines of the same sizes. Though it seems that the curves do not follow the same shape and trend as the Wiseman engine, their respective Pearson coefficients suggest that the data fits very close to the power curve, since they all have an $R^2 > 0.97$.

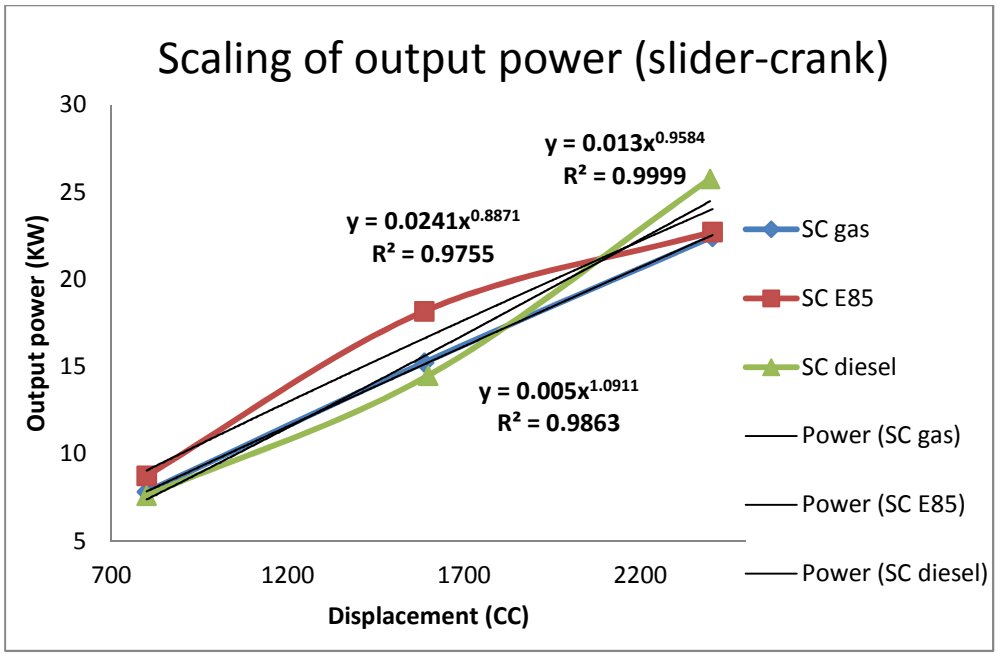

Figure 44 - Scaling Slider-crank Engine's Peak Power with Size at 2000 RPM

The trend can further compared between the slider-crank and Wiseman variants like torque comparison to see how they perform against each other in terms of output power when operating on different fuels.

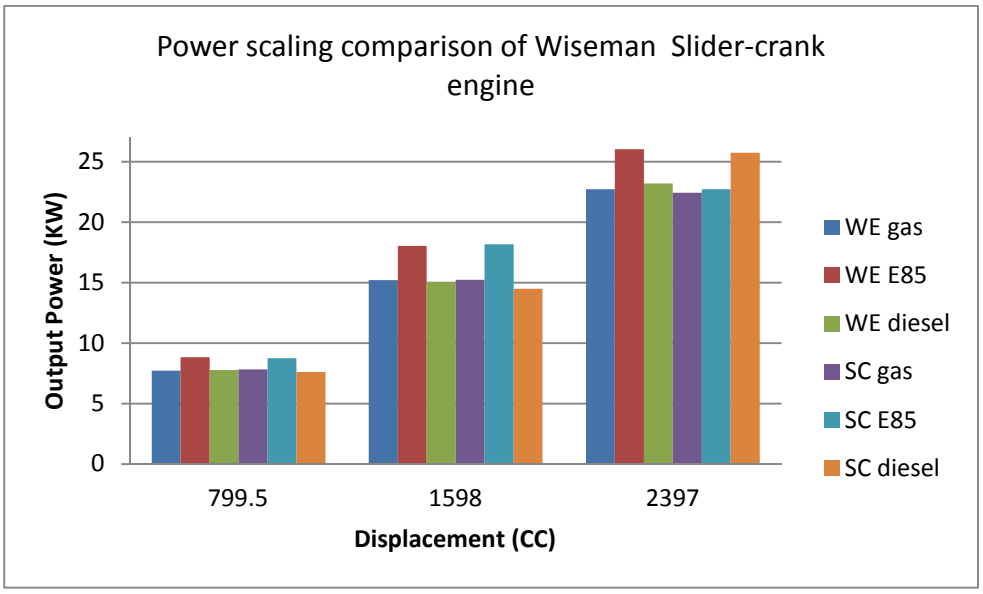

Figure 45 - Comparing the Scaled Power of Wiseman and Slider-crank Engine

The comparison in Figure 45 shows that the Wiseman variants tend to produce more power than its slider-crank counterparts irrespective of the fuel used. This is true especially true for the 30 HP (2397 cc) variant using E85 fuel. On the contrary, the 30 HP slider-crank diesel engine produces more power compared to Wiseman engine of same size. And the difference between the power produced by the Wiseman and slider-crank versions operating on gas is insignificant.

IV. Scaling the Engine Fuel Consumption at Peak Power Output

It was noted from Mr. Menon's findings that when it comes to the fuel consumption of an engine, miniature engines tend to have a greater drop in fuel efficiency as the size of the engine decreases compared to the engines of conventional sizes. The reason stated for this trend is because smaller engines tend to have higher losses. This means that as the engine size increases, the fuel efficiency slightly increases as seen in Figure 46.

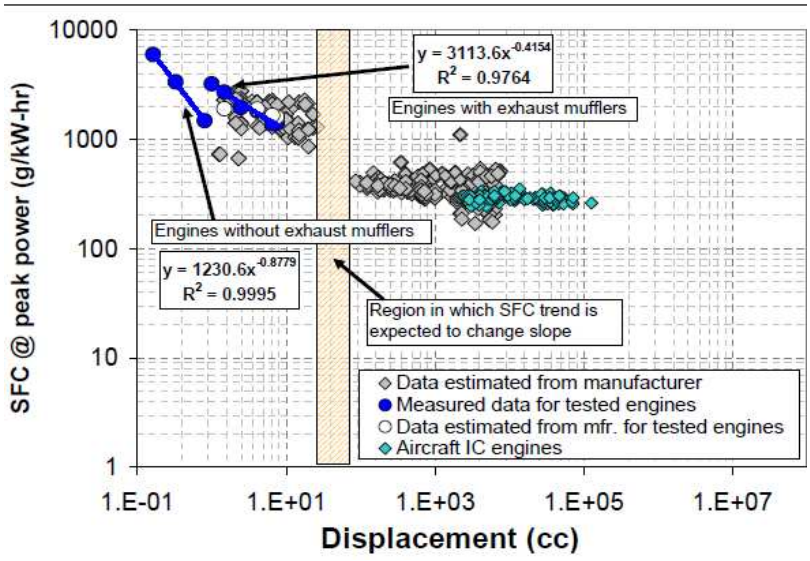

Figure 46 - Scaling of SFC at Peak Power with Engine Size (Menon, 2010)

It can be observed that the engines had a steeper slope for fuel consumption for sizes until 15 cc but in the region of 15-20 cc this trend in the slope changes (Menon, 2010). Engines that share the same range of displacement as the Wiseman prototypes, 800-2500 cc, tend to have a gradual increase in the fuel efficiency with increase in engine size.

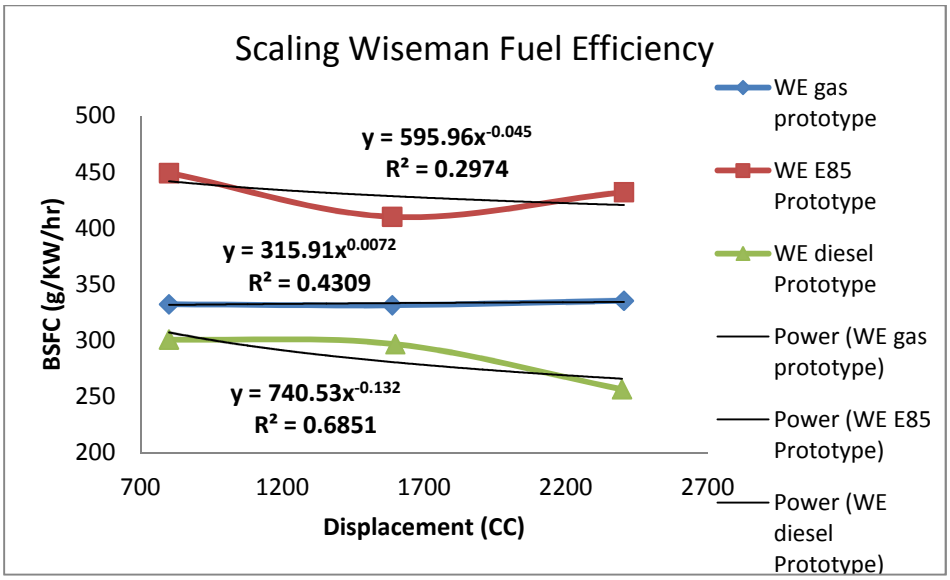

Figure 47 - Scaling Wiseman Engine's BSFC with Respect to Engine Displacement

As seen in Figure 47, the Wiseman prototypes show a similar trend as the fuel efficiency law established earlier, but the approach does not seem to be very effective considering the lower values of R^2. This shows that the data does not fit very well with the implemented power curve. The fuel efficiency of the engines mostly varies with the change in the displacement but overall there is a slight improvement with the increase in engine displacement. Similar to the results from previous multi-fuel tests, the engines operating on E85 tend to consume more fuel in general than while operating on gas and diesel. This could again be due to the

lower calorific value of the E85 fuel. Again, the diesel Wiseman engines seem to be the most promising in terms of fuel efficiency, with the 30 HP variant showing the best results. It was also noted that the gas variants did not show any significant change in the fuel efficiency with change in displacement.

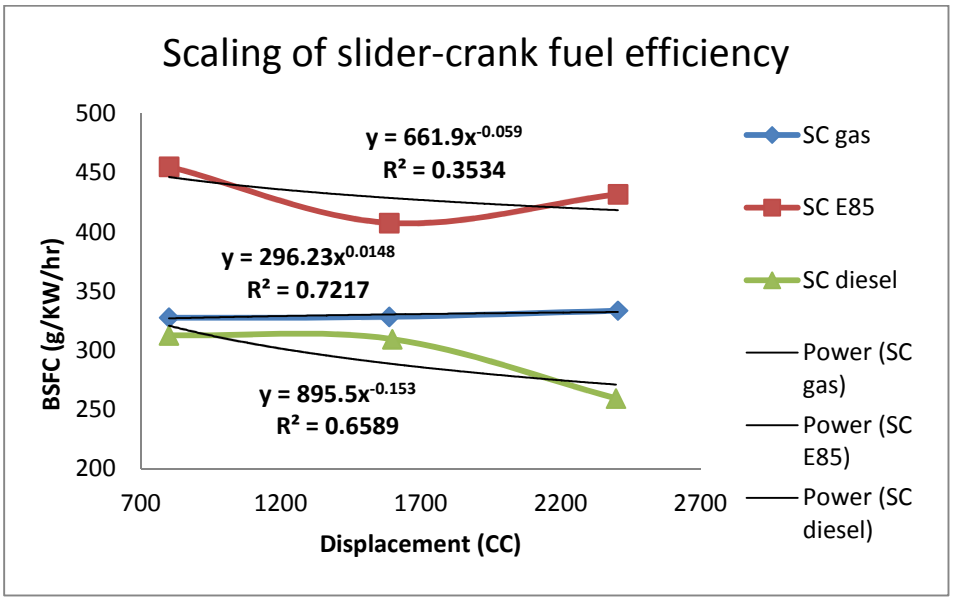

Figure 48 - Scaling Slider-crank Engine's BSFC with Respect to Engine Size

The Slider-crank versions of the Wiseman engines also show exactly same trend, as seen in Figure 48. They too tend to have slightly lower fuel consumption as the engine's displacement increases. Again, the change is very stable in the gas engines while the diesel engines prove to be most fuel efficient. The E85 variants again show high fuel consumption. This data was further compared to see how the engines with Wiseman mechanism perform in terms of fuel efficiency when compared to the slider-crank versions of the same size.

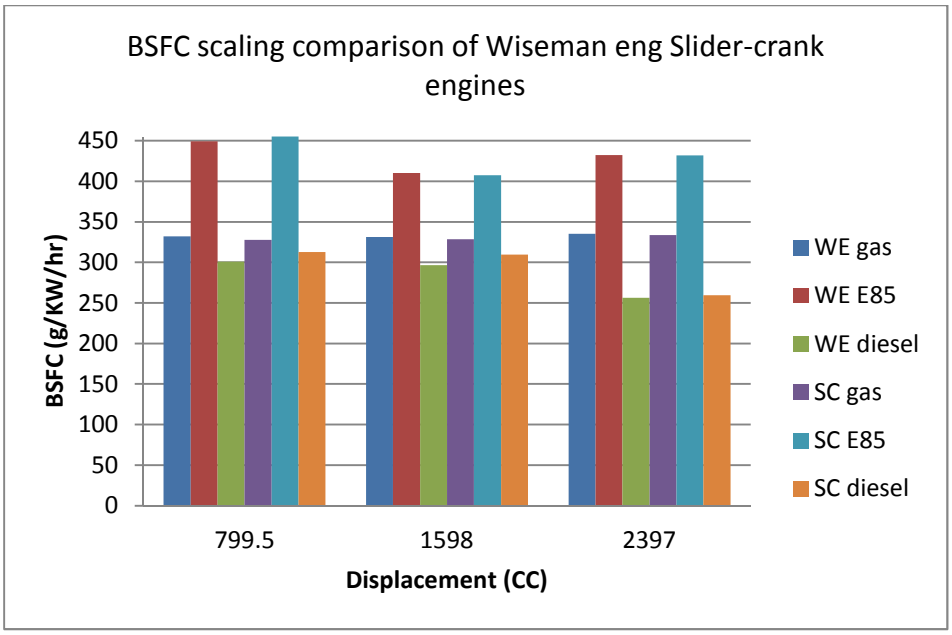

Figure 49 - Comparing the Scaled BSFC of Wiseman and Slider-crank Engine

From the comparison of the BSFC results in Figure 49, it can be seen that the Wiseman engines of the same size as the slider-crank engines tends to be slightly less fuel efficient but the difference is almost negligible. Though both the engines follow a common trend, i.e. increase in fuel efficiency with increase in engine displacement. The gas and E85 variants of both the engines have almost identical fuel consumption. The Wiseman diesel engines prove to be a little more fuel efficient than the slider-crank engines of the same displacement.

V. Scaling the Engine Brake Mean Effective Pressure (BMEP)

Another important engine parameter to gauge the engine's performance is the BMEP. The BMEP decides the work done by the piston which in turn determines the output torque and power. This reflects on the overall quality of the engine design. From the research findings of Mr. Menon it was stated that the

engine BMEP gradually increase with increase in engine displacement (Figure 50). Though it is important to note that his results did not have a very good fit with $R^2 \sim 0.5$ (Menon, 2010). It should also be noted that the engine BMEP was not measured at a constant speed but instead the peak BMEP was recorded (generally at very low speeds).

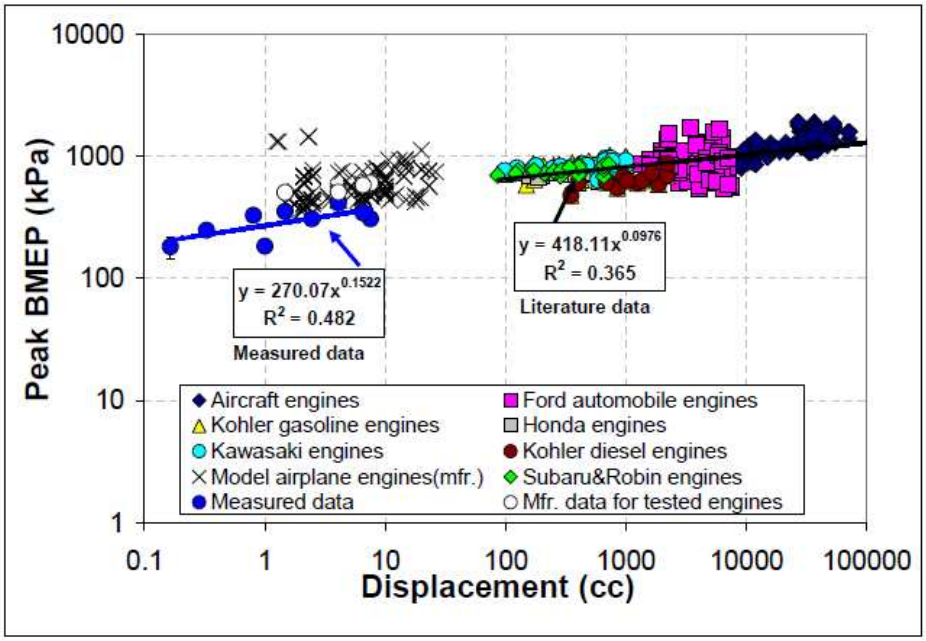

Figure 50 - Scaling of Peak Engine BMEP with Engine Size (Menon, 2010)

Figure 51 also shows a similar trend in the peak BMEP of the Wiseman engines with respect to their engine displacements. Though the trend is not clearly recognizable from the plots, due to the small size of the data set, overall the BMEP seems to increase with increase in cylinder displacement. The scaling law seems most evident in the gas variants of the engines, whereas the diesel engines tend to show the opposite trend. It can also be seen that the engines operating on E85 fuel produces more BMEP than the gas versions in general. This is especially

true in the case of 30 HP design operating on E85 since it shows the highest BMEP output. This trend was also noticed while comparing the performance of the Wiseman 30 cc engine while operating on gas and E85. Another observation that can be made is that the 20 HP engines operating on E85 has a lower BMEP output than the 20 HP diesel engines.

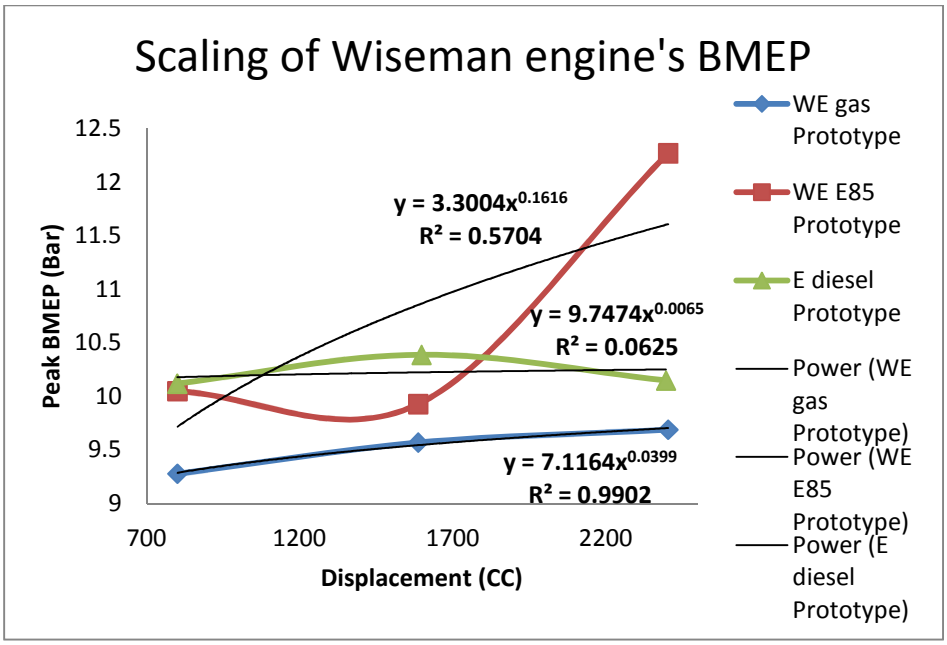

Figure 51 - Scaling Wiseman Engine's BMEP with Respect to Engine Displacement

In case of scaling the slider-crank versions of the same engines, it seems that the engines running on gas and E85 have an gradual increase in the cylinder BMEP while the diesel variants tends to follow a trend more similar to the E85 version of the Wiseman engine. This can be seen in Figure 52. The ethanol engines still produce higher BMEP than its gas counterparts, while the 30 HP version of the diesel engine produces best result of them all.

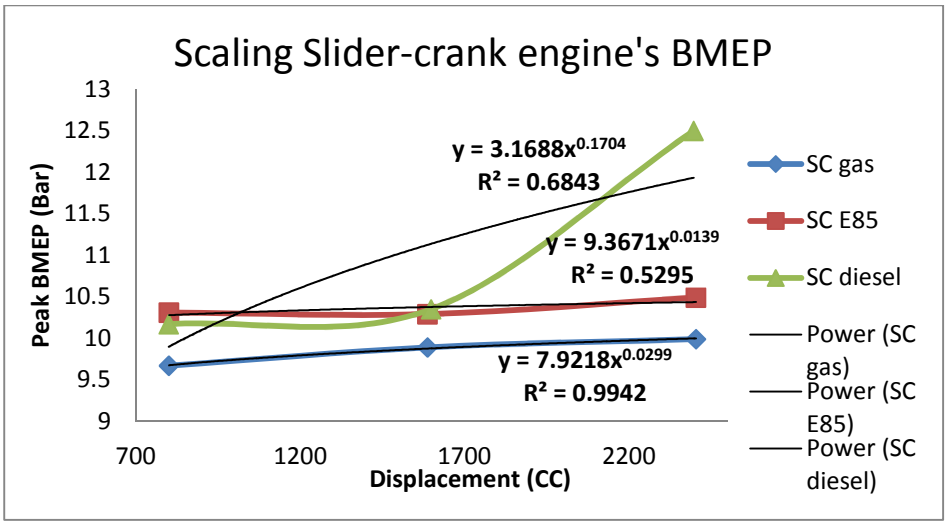

Figure 52 - Scaling Slider-crank Engine's BMEP with Respect to Engine Size

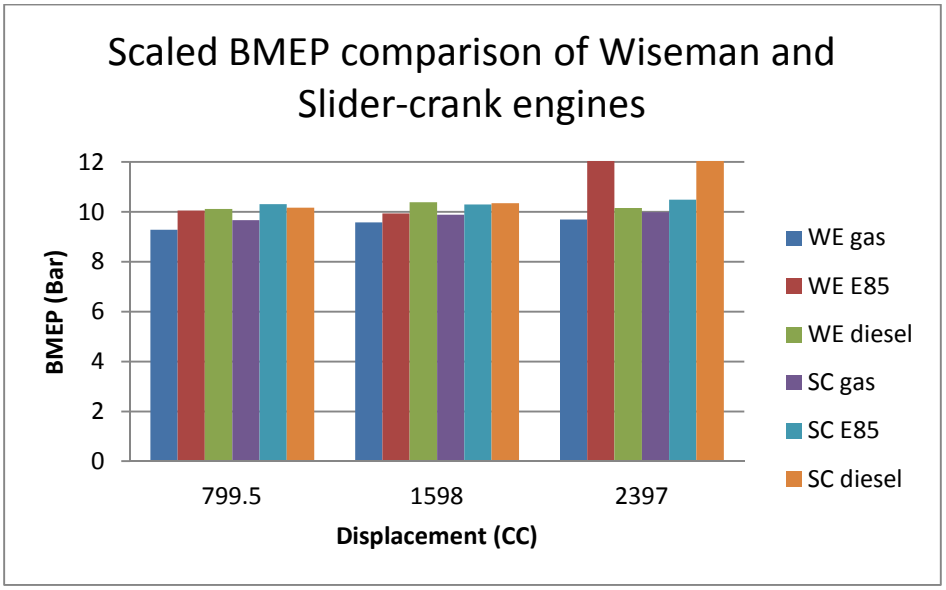

Figure 53 - Comparing the Scaled BMEP of Wiseman and Slider-crank Engine

While comparing the cylinder BMEP of the Wiseman and slider-crank engines with respect to their cylinder size in Figure 53, it can be observed that the slider-crank engines have a higher BMEP output than the Wiseman engines in general. There are two exceptions to this trend and both are for the 30 HP variants

of these engines. The 30 HP slider-crank diesel and 30 HP Wiseman ethanol variants produce almost identical BMEP. The BMEP of these two engines is also the highest out of all the engines.

Chapter 6

CONCLUSION AND RECOMMENDATIONS

The heat engine comprising of the slider-crank mechanism has been the popular choice in the market till date. Though there have been other engines but none of them have seen the level of commercial success as the slider-crank mechanism. Despite being popularly implemented, the slider-crank mechanism has few design limitations. It tends to have loss of energy in the form of heat generated by friction. The main source of this friction is due to the piston rubbing against the cylinder wall during its motion. Most engine designers focus on how to minimize the loss of energy due to internal friction in the engine which in turn will increase the overall efficiency of the engine.

An alternative mechanism was proposed by Wiseman Inc., which utilized the geared hypocycloid concept by replacing the conventional crankshaft in the engine. The idea of using hypocycloidal gear assembly in a combustion engine is centuries old but it has never been commercially implemented. The assembly consists of a pinion gear which rotates inside a ring gear. By making the gear ratios to 2:1, every point on the parameter of the pinion gear provides a straight line curve, and this benefits the piston motion in ICE. The connecting rod and the piston when connected to such a point on the pinion gear, has a straight line motion. This means that the piston has a perfect sinusoidal motion and there is no friction between it and the cylinder walls. The Wiseman design takes advantage of this phenomenon in their patented design for a 30 cc engine. Other than the advantage of reduced friction, a hypocycloid engine also has tends to be dimensionally smaller and is believed to have higher performance outputs than a

conventional slider crank engine of the same size. Theoretically, the reason behind better performance is that the straight line motion eliminates bending of the connecting rod due to the gas force which contributes to better utilization of the gas force. This means more work is done per every stroke, resulting in higher torque and power. Though, it has not been proved to be more fuel efficient.

Previous studies have proved these claims to be true to an extent but a more detailed study was necessary. In order to thoroughly analyze the Wiseman engine's performance when compared to a conventional slider-crank engine of the same size, it was thought wise to use the Lotus Engine Simulation software. The authenticity of the results produced by the LES software was validated by first simulating the performance of a stock engine with known parameters and comparing the results with the manufacturer provided specifications. From the output comparison of the results generated by LES software and that provided by the manufacturer, it was concluded that the software results were reliable provided all minor details of the engine are taken into consideration. This approach seems logical since by providing more details, a more realistic operating situation is created during the simulation. Further, a detailed Wiseman 30 cc engine was modeled in the LES software along with its unique piston motion and the simulated results were compared with the same engine having a conventional slider-crank piston motion. It was noticed that the Wiseman engine produced slightly lower power (0.83 HP) than the slider-crank engine (0.89 HP) at the peak engine speeds (6000 RPM). Though the peak output power of the Wiseman engine was much closer to the designed peak power of 0.99 HP. This meant that the Wiseman engine produced about 7% less power than the slider crank engine. A similar trend was also observed during

previous dynamometer tests conducted on the Wiseman engine. Contradictory to the theoretical expectations, the Wiseman 30 cc engine had a lower torque output than the slider-crank engine while being about 6% less fuel efficient. Prior tests by Wiseman Inc. claimed that the engine was about twice as fuel efficient than its slider-crank variant.

Another study on the Wiseman engine was conducted to observe how the Wiseman engine would perform if a 4 stroke diesel version was designed. The simulated results for this variant of the engine proved to be very promising in almost all aspects. It was seen that a 30 cc four stroke Wiseman diesel engine, produced higher power and torque than the 2 stroke Wiseman and slider-crank engines running on gas. The reason behind it is that the 4 stroke fuel injected engine had a higher volumetric efficiency, which meant it utilized the air and fuel mixture in an optimum manner. This further reflected in fuel consumption comparisons, where the 4 stroke Wiseman diesel engine proved to be a lot more fuel efficient than the 2 stroke gas engines.

Further, the Wiseman engine was analyzed to see its multi-fuel capabilities if a contra piston were incorporated in the design. For the sake of this study, the performance of the 2 stroke Wiseman engine was tested using different fuels while its compression ratio was changed. It was noticed that the Wiseman engine while operating on E85 flex-fuel performed better in terms of power and torque than while running on pure gasoline. It was noted that the engine produced about 1.4% more power while operating on E85. The properties of E85 as an engine fuel along with the implementation of higher compression ratio contributed to this improved performance. However, the fuel efficiency of the engine plummeted significantly while it operated on E85. The reason behind this is that, E85 has significantly lower calorific value than gasoline, which means the engine

while operating on E85 requires more energy (fuel) to perform the same amount of work as gasoline engine.

The current 30 cc Wiseman engine produces less than 1 HP and so to expand its range of applications in future, more powerful engine designs were required. For this purpose, 4 stroke Wiseman engines with power outputs of 10 HP, 20HP and 30 HP were designed. Since these engines were only theoretical prototypes, it was necessary to study how their performance would change with respect to their size. Increase in engine power also meant an increase in engine displacement, and so a performance scaling analysis was conducted to predict how the output power, torque and fuel efficiency would change according to the displacement while operating on different fuels. The analysis involved using previously established scaling laws for each parameter to study the trend. It was noticed that as the engine displacement increased, the torque and the power produced by it also increased. This was true for a slider-crank as well as an engine using Wiseman mechanism. The engines operating on E85 fuel produced higher torque especially for the 30 HP design. This was true for both, the Wiseman engine and a slider-crank engine of the same size. In case of power, the 30 HP Wiseman engine produce more power than a 30 HP slider-crank diesel engine. Overall, it was noticed that the Wiseman engines fared better in terms of power and torque than the slider-crank engines as the size increased. A similar trend was also noticed when it came to engine fuel consumption with respect to its size. It was observed that as the engine's displacement increased, it became more fuel efficient. A reason for this is that smaller engines tend to have higher motoring losses. While comparing this trend with slider-crank engines, it was found that the 30 HP Wiseman engine while operating on diesel had the best fuel efficiency. Further, the

change in engine's BMEP was studied and it was found that as the cylinder displacement increased, the BMEP also increased. Once again, the 30 HP Wiseman design produced the highest BMEP as compared all the other engines. Though the difference between that engine and a conventional 30 HP diesel engine was negligible.

From all the analysis conducted, it can be concluded that the simulated results by LES software for 30 cc Wiseman engine are comparable to those obtained by previous dynamometer tests. Though, these results are not favorable when compared to an engine using the slider-crank mechanism. There needs to be additional tuning done in order to optimize the performance of the 30 cc Wiseman engine. The scaling and multi-fuel analysis suggests that the 4 stroke diesel and ethanol variants of the Wiseman engine seem more promising than the 2 stroke gasoline engine. It would also benefit to explore and develop the 30 HP diesel and ethanol designs since the simulated results for those engines are most optimum. These engines also showed a closer relationship to the trend where the increase in HP increases the displacement which in turn increases the output torque. It was also found that increasing the HP reduces the fuel consumption for the amount of power generated.

Recommendations and Future Work

To further develop a multi-fuel Wiseman engine there are some key factors that need to be taken into consideration. Since, the proposed contra piston design operates on variety of fuels including ethanol, it should be noted that ethanol like other alcohols is corrosive in nature and over time it might damage the engine's components like spark plugs. It should also be noted that as the concentration of the ethanol in the fuel increases,

engine components like fuel filter, fuel pump, ignition system and the exhaust system need to be modified for trouble free performance. The orifice diameters also need to be increased for the engines operating on ethanol to allow proper mixing of air and fuel depending on varying engine speeds. Having high compression ratio for ethanol and diesel engines also means higher loads on the bearings and the connecting rod, which might result in component failure. It would also benefit to study Wiseman engines designs for HP between the intervals of 10, 20 and 30 so a stronger relationship with the scaling laws can be established.

REFERENCES

Ganesan, V. (2012). *Internal combustion engines*. (4th ed.). New Delhi: Tata McGraw Hill Education Pvt. Ltd.

Bai, D., Solving piston secondary motion of internal combustion engines. *Sloan Automotive Laboratory*, Retrieved from http://math.mit.edu/classes/18.086/2008/final_report_dongfang_bai.pdf

Mathur, M. L., & Sharma, R. P. (1997). *A course in internal combustion engines*. (7th ed.). New Delhi: Dhanpat Rai Publications Pvt. Ltd.

H. W. Dickinson, "James White and His 'New Century of Inventions", Transactions of the Newcomen Society, 1949-1951, vol. 27, pp. 175-179.

James White, A New Century of Inventions, Manchester, 1822, pp. 30-31, 338. A hypocycloidal engine used in Stourbridge, England, is in the Henry Ford Museum

Karhula, J. (2008). *Cardan Gear Mechanism versus Slider Crank Mechanism in Pumps and Engines.* Lappeenranta: Lappeenranta University of Technology.

Wolfram MathWorld. (2010, October). Retrieved from Hypocycloid: http://mathworld.wolfram.com/Hypocycloid.html

Polly Model Engineering Limited. (2010, October). Retrieved from Stationary Engine Kits: http://www.pollymodelengineering.co.uk/sections/stationary-engines/anthony-mount-models/murrays-Hypocycloidal-Engine.asp

Special plane curves. (2005-2014). Retrieved from http://www.math10.com/en/geometry/analytic-geometry/geometry5/special-plane-curves.html

Conner, T. (2011). "Critical Evaluation and Optimization of a Hypocycloid Wiseman Engine", M.S. Thesis, Arizona State University, 2011.

Wiseman Engine Group. (2010). *The engine of the future - today!* Business Plan.

Wiseman Technologies, Inc. (n.d.). Retrieved from UAV Design: http://www.wisemanengine.com/AUVSIWisemanPaPer.doc

Wiseman, R. (2001). *Patent No. 6,510,831*. United States of America.

Taylor, C.F., The Internal Combustion Engine in Theory and Practice. Volume 2: Combustion, Fuels, Materials, Design, Revised Edition. The M.I.T. Press, Massachusetts Institute of Technology, Cambridge, Massachussets, 1985

Beachley, N. H., & Lenz, M. A. (1988). A Critical Evaluation of the Geared Hypocycloid Mechanism for Internal Combustion Engine Application". *Scociety of Auotmotive Engineers, Inc*

Ishida, K., & Matsuda, T. (1975). Fundamental Researches on a Perfectly Balanced Rotation-Reciprocation Mechanism. *Bulletin of the JSME* , 185-192.

Ruch, David M., "An Experimental and Analytical Investigation of a Single-Cylinder Modified Hypocycloid Engine Design," PhD dissertation, University of Wisconsin at Madison, 1992

Menz, K.C., "Design and Experimentation of a 'Big Bearing' Internal Geared Hypocycloid Air Compressor," M.S. Thesis, University of Wisconsin-Madison, 1987.

A Combustion Correlation for Diesel Engine Simulation. N.Watson, A.D.Pilley & M.Marzouk. SAE 800029.

Investigation of Internal Combustion Engine Problems. G.Eichelberg "Engineering Oct 1939 Vol 148, 463 & 547"

Heat Transfer in the Cylinder of Reciprocating Internal Combustion Engines. W.J.D.Annand (Proc.I.Mech.E 177.973 (1963))

American coalition for ethanol. (n.d.). Retrieved from http://ethanol.org/index.php?id=50&parentid=8

U.S. Department of Energy, Energy Efficiency & Renewable Energy. (2013). *Handbook for handling, storing, and dispensing e85 and other ethanol-gasoline blends*. Retrieved from U.S. Department of Energy website: http://www.afdc.energy.gov/uploads/publication/ethanol_handbook.pdf

Costa, R. C., & Sodre, J. R. (2010). Hydrous ethanol vs. gasoline-ethanol blend: Engine performance and emissions. *Fuel, 89*(2), 287-293. Retrieved from http://www.sciencedirect.com/science/article/pii/S0016236109002981

Costa, R. C., & Sodre, J. R. (2010). Compression ratio effects on an ethanol/gasoline fuelled engine performance. *Applied Thermal Engineering,21*(2-3), 278-283. Retrieved from http://ac.els-cdn.com/S1359431110003947/1-s2.0-S1359431110003947-main.pdf?_tid=7912e454-af24-11e3-9135-00000aacb361&acdnat=1395205873_1452066f302a7ab8e1c47b99a6859ba3

Cahyono, B., & Bakar, R. A. (2010). Effect of ethanol addition in the combustion process during warm-ups and half open throttle on port-injection gasoline engine. *American Journal of Engineering and Applied Sciences*, *4*(1), 66-69. doi: 10.3844/ajeassp.2011.66.69

Datta, A., Chowdhuri, A. K., & Mandal, B. K. (2012). Experimental study on the performances of spark ignition engine with alcohol-gasoline blends as fuel.*International Journal of Energy Engineering*,*2*(1), 22-27.

Celik, M. B., & , (2007). Experimental determination of suitable ethanol–gasoline blend rate at high compression ratio for gasoline engine. *Applied Thermal Engineering*, *28*(5-6), 396-404. doi: 10.1016/j.applthermaleng.2007.10.028

Topgul, T., Yucesu, H. S., Cinar, C., & Koca, A. (2006). The effects of ethanol–unleaded gasoline blends and ignition timing on engine performance and exhaust emissions. *Renewable Energy*, *31*(15), 2534-2542. Retrieved from http://www.sciencedirect.com/science/article/pii/S0960148106000401

Kale. *Theory of engine design*.

Lotus Cars Ltd. (2001). Getting Started Using Lotus Engine Simulation Ver 5.05.

Zhai, H., Frey, H. C., Rouphail, N. M., Gonsalves, G. A., & Farias, T. L. (2007, June). *Fuel consumption and emissions comparisons between ethanol 85 and gasoline fuels for flexible fuel vehicles*. 100th annual meeting of the air & waste management association, Pittsburgh, PA.

Menon, S. K. (2006). *Performance measurement and scaling in small internal combustion engines.*. (Master's thesis, University of Maryland).

Menon, S. (2010). *The scaling of performance and losses in miniature internal combustion engines.*. (Doctoral dissertation, University of Maryland).

APPENDIX A

COMMON LES SOFTWARE TEST CONDITIONS

Steady State Test Conditions	
Ambient Air Pressure (bar abs.)	1.01
Ambient Air Temperature (C)	20
Inlet Pressure (bar abs.)	1.01
Inlet Temperature (C)	20
Exit Pressure (bar abs.)	1.01
Equivlance Ratio	1.1
Specific Humidity	0.00

Piston Motion (User Sub. Id No.)	
Slider Crank	1000
Wiseman Engine	3000

Fuel			
Fuel System	Carburettor	Indirect Injection	Direct Injected
Fuel Type	Gasoline	Diesel	Ethanol
Calorific Value (kJ/kg)	43000	42700.00	28765
Density (kg/liter)	0.75	0.84	0.782
H/C Ratio Fuel (molar)	1.800	1.90	2.7177
O/C Ratio Fuel (molar)	0.00	0.00	0.3951
Molecular Mass (kg/k.mol)	114.23	170.00	46
Maldistribution Factor	1.000	1.000	1.000

APPENDIX B

30 cc LES MODEL INPUT PARAMETERS

Intake	
Total length (mm)	10.00
No. of Diameters	2
Start diameter (mm)	6
End diameter (mm)	6
Pipe Volume (l)	.0003
Surface area (mm^2)	1.8850e+002
No. of meshes	2
Wall thickness (mm)	1.000
Cooling Type	Air Cooled
Temperature (C)	20
Ext. HTC ($W/m^2/K$)	20
Wall material	Aluminum

Intake disk valve	
Disk valve option	Standard
Valve Dia. (mm)	120
Port Dia. (mm)	10
Valve open (deg)	24
Valve Close (deg)	290
Max Area CD Coeff	0.99

Inlet Variable Volume Plenum	
Equiv. Bore (mm)	35.94
Equiv. Stroke (mm)	28.45
Equiv. Rod Length (mm)	56.00
Equiv Compression Ratio (PCR)	1.60
TDC Angle (deg)	180
Wall Temperature (C)	100
Plenum HTC ($W/m^2/K$)	5.00
Speed Ratio	1.000

Piston Ported Intake Valve	
Valve Option	Standard
Port Width (mm)	40.00
Max. Port Height (mm)	2.00
Stroke (mm)	28.45
Rod Length (mm)	56.00
Valve Open (deg)	124.00
Max Area CD Coeff	0.900

Cylinder	
Bore (mm)	35.94
Stroke (mm)	28.45
Cyl Swept Volume (l)	.02886
Total Swept Volume (l)	.02866
Con-rod Length (mm)	56.00
Pin Off-Set (mm)	0
Compression Ratio	8
Clearance Volume (l)	.004123
Phase (ATDC)	0.00

Piston Ported Exhaust	
Port Width (mm)	20.82
Max. Port Height (mm)	7.41
Stroke (mm)	28.45
Rod Length (mm)	56.00
Valve Open (deg)	108.00
Max Area CD Coeff	0.900

Exhaust pipe	
Total Length (mm)	30.00
No. of diameters	2
Start diameter (mm)	11.00
End Diameter (mm)	11.00
Pipe Volume (l)	.0029
Surface Area (mm^2)	1.0367e+003
No. of Meshes	2
Wall Thickness (mm)	1.000
Cooling Type	Air Cooled
Temperature (C)	20.00
Ext. HTC ($W/m^2/K$)	20.00
Wall Material	Aluminum

APPENDIX C

30 cc DIESEL LES MODEL INPUT PARAMETERS

Intake area to plenum	
Throttle Type	Simple Area
Discharge Data Type	CF Fixed Value
Discharge Directionality	Common
Discharge CF	1.00
Minimum C.S.A (mm^2)	28.33
Equivalent Diameter (mm)	3.006

Single intake plenum	
Volumt (litres)	0.0289
Surface Area (mm^2)	4.5503e+003
Wall Temperature (^oC)	20.00
Plenum HTC ($W/m^2/K$)	0.00

Intake port	
No. of Valves	1
Valve Throat Dia (mm)	17.236
Port Type	User Curve (common)

Intake Valve	
Valve Open (deg)	12.00
Valve Close (deg)	58.00
Dwell at Max (deg)	0.0
Max Lift (mm)	5.602
MOP (deg)	113.00
Lift Option	User Specified Valve Lift
Data Action	Scale

Cylinder	
Bore (mm)	35.94
Stroke (mm)	28.45
Cyl. Swept Volume (l)	0.02886
Total Swept Volume (l)	0.02886
Con-rod Length (mm)	56
Pin Off-set (mm)	0.00
Compression Ratio	17
Clearance Volume (l)	0.001804

Exhaust Valve	
Valve Open (deg)	58.00
Valve Close (deg)	12.00
Dwell at Max (deg)	0.0
Max Lift (mm)	5.602
MOP (deg)	-113.00
Lift Option	User Specified Valve Lift
Data Action	Scale

Exhaust port	
No. of Valves	1
Valve Throat Dia (mm)	14.421
Port Type	User Curve (common)

Single exhaust plenum	
Volumt (litres)	0.0115
Surface Area (mm^2)	2.4703e+003
Wall Temperature (^oC)	500.00
Plenum HTC ($W/m^2/K$)	0.00

Exit area from plenum	
Throttle Type	Simple Area
Discharge Data Type	CF Fixed Value
Discharge Directionality	Common
Discharge CF	1.00
Minimum C.S.A (mm^2)	26.59
Equivalent Diameter (mm)	5.819

APPENDIX D

GUNT LES MODEL INPUT PARAMETERS

Intake area to plenum	
Throttle Type	Simple Area
Discharge Data Type	CF Fixed Value
Discharge Directionality	Common
Discharge CF	1.00
Minimum C.S.A (mm^2)	178.07
Equivalent Diameter (mm)	15.057

Single intake plenum	
Volumt (litres)	0.3486
Surface Area (mm^2)	2.3872e+004
Wall Temperature (^oC)	25
Plenum HTC ($W/m^2/K$)	0.00

Intake port	
No. of Valves	1
Valve Throat Dia (mm)	19
Port Type	User Curve (common)

Intake Valve	
Valve Open (deg)	49.00
Valve Close (deg)	74.00
Dwell at Max (deg)	0.0
Max Lift (mm)	9.625
MOP (deg)	102.48
Lift Option	Slow Lift Polynomial

Cylinder	
Bore (mm)	80.00
Stroke (mm)	69.00
Cyl. Swept Volume (l)	0.34683
Total Swept Volume (l)	0.34683
Con-rod Length (mm)	103.00
Pin Off-set (mm)	0.00
Compression Ratio	21.50
Clearance Volume (l)	0.016919

Exhaust Valve	
Valve Open (deg)	76.00
Valve Close (deg)	39.00
Dwell at Max (deg)	0.0
Max Lift (mm)	9.625
MOP (deg)	-108.52
Lift Option	Slow Lift Polynomial

Exhaust port	
No. of Valves	1
Valve Throat Dia (mm)	19.10
Port Type	User Curve (common)

Single exhaust plenum	
Volumt (litres)	0.1387
Surface Area (mm^2)	1.2960e+004
Wall Temperature (^oC)	500.00
Plenum HTC ($W/m^2/K$)	0.00

Exit area from plenum	
Throttle Type	Simple Area
Discharge Data Type	CF Fixed Value
Discharge Directionality	Common
Discharge CF	1.00
Minimum C.S.A (mm^2)	164.34
Equivalent Diameter (mm)	14.465

APPENDIX E

10 HP/ 20 HP/ 30 HP GASOLINE AND ETHANOL MODEL INPUT PARAMETERS

Intake area to plenum	
Throttle Type	Simple Area
Discharge Data Type	CF Fixed Value
Discharge Directionality	Common
Discharge CF	1.00
Minimum C.S.A (mm^2)	224.36/ 448.71/ 673.07
Equivalent Diameter (mm)	16.902/ 23.902/ 29.274

Single intake plenum	
Volumt (litres)	0.80/ 1.60/ 2.40
Surface Area (mm^2)	4.1675e+004/ 6.6155e+004/ 8.6688e+004
Wall Temperature (^oC)	20/ 20/ 20
Plenum HTC ($W/m^2/K$)	0.00

Intake port	
No. of Valves	1
Valve Throat Dia (mm)	26/ 40.504/ 53.00
Port Type	Default Poor Port

Intake Valve	
Valve Open (deg)	12.00/ 12.00/ 12.00
Valve Close (deg)	58.00/ 58.00/ 58.00
Dwell at Max (deg)	0.0
Max Lift (mm)	9.625/ 9.625/ 9.625
MOP (deg)	113.00/ 113.00/ 113.00
Lift Option	Fast Lift Polynomial

Cylinder	
Bore (mm)	94.67/ 119.44/ 134.87
Stroke (mm)	113.64/ 142.80/ 168.00
Cyl. Swept Volume (l)	0.79992/ 1.59999/ 2.40010
Total Swept Volume (l)	0.79992/ 1.59999/ 2.40010
Con-rod Length (mm)	170.46/ 214.20/ 252.00
Pin Off-set (mm)	0.00
Compression Ratio	8 (Gas) & 13 (Ethanol)
Clearance Volume (l)	0.114274/ 0.228570/ 0.342872

Exhaust Valve	
Valve Open (deg)	58.00/ 58.00/ 58.00
Valve Close (deg)	12.00/ 12.00/ 12.00
Dwell at Max (deg)	0.0
Max Lift (mm)	9.625/ 9.625/ 9.625
MOP (deg)	-113.00/ -113.00/ -113.00
Lift Option	Fast Lift Polynomial

Exhaust port	
No. of Valves	1
Valve Throat Dia (mm)	22.00/ 33.888/ 42.00
Port Type	Default Poor Port

Single exhaust plenum	
Volumt (litres)	0.32/ 0.64/ 0.96
Surface Area (mm^2)	2.2625e+004/ 3.5915e+004/ 4.7061e+004
Wall Temperature (^oC)	500.00/ 500.00/ 500.00
Plenum HTC ($W/m^2/K$)	0.00

Exit area from plenum	
Throttle Type	Simple Area
Discharge Data Type	CF Fixed Value
Discharge Directionality	Common
Discharge CF	1.00
Minimum C.S.A (mm^2)	210.59/ 421.19/ 631.78
Equivalent Diameter (mm)	16.375/ 23.158/ 28.362

APPENDIX F

10 HP/ 20 HP/ 30 HP DIESEL MODEL INPUT PARAMETERS

Intake area to plenum	
Throttle Type	Simple Area
Discharge Data Type	CF Fixed Value
Discharge Directionality	Common
Discharge CF	1.00
Minimum C.S.A (mm^2)	224.36/ 448.71/ 673.07
Equivalent Diameter (mm)	16.902/ 23.902/ 29.274

Single intake plenum	
Volumt (litres)	0.80/ 1.60/ 2.40
Surface Area (mm^2)	4.1675e+004/ 6.6155e+004/ 8.6688e+004
Wall Temperature (^oC)	20/ 20/ 20
Plenum HTC ($W/m^2/K$)	0.00

Intake port	
No. of Valves	1
Valve Throat Dia (mm)	24/ 34.00/ 41.00
Port Type	Default Poor Port

Intake Valve	
Valve Open (deg)	12.00/ 12.00/ 12.00
Valve Close (deg)	58.00/ 58.00/ 58.00
Dwell at Max (deg)	0.0
Max Lift (mm)	9.625/ 9.625/ 9.625
MOP (deg)	113.00/ 113.00/ 113.00
Lift Option	Fast Lift Polynomial

Cylinder	
Bore (mm)	93.41/ 117.70/ 134.73
Stroke (mm)	116.75/ 147.06/ 168.35
Cyl. Swept Volume (l)	0.80008/ 1.60006/ 2.40011
Total Swept Volume (l)	0.80008/ 1.60006/ 2.40011
Con-rod Length (mm)	175.13/ 220.59/ 252.53
Pin Off-set (mm)	0.00
Compression Ratio	16
Clearance Volume (l)	0.053339/ 0.106671/ 0.160008

Exhaust Valve	
Valve Open (deg)	58.00/ 58.00/ 58.00
Valve Close (deg)	12.00/ 12.00/ 12.00
Dwell at Max (deg)	0.0
Max Lift (mm)	9.625/ 9.625/ 9.625
MOP (deg)	-113.00/ -113.00/ -113.00
Lift Option	Fast Lift Polynomial

Exhaust port	
No. of Valves	1
Valve Throat Dia (mm)	20.00/ 33.00/ 41.00
Port Type	Default Poor Port

Single exhaust plenum	
Volumt (litres)	0.32/ 0.64/ 0.96
Surface Area (mm^2)	2.2625e+004/ 3.5915e+004/ 4.7061e+004
Wall Temperature (^oC)	500.00/ 500.00/ 500.00
Plenum HTC ($W/m^2/K$)	0.00

Exit area from plenum	
Throttle Type	Simple Area
Discharge Data Type	CF Fixed Value
Discharge Directionality	Common
Discharge CF	1.00
Minimum C.S.A (mm^2)	210.59/ 421.19/ 631.78
Equivalent Diameter (mm)	16.375/ 23.158/ 28.362